Hot-spring inputs and climate drive dynamic shifts in archaeal communities in Lake Magadi, Kenya Rift Valley

Evan R. Collins[1], Troy M. Ferland[2], Isla S. Castañeda[3], R. Bernhart Owen[4], Tim K. Lowenstein[5], †Andrew S. Cohen[6], Robin W. Renaut[7], Molly D. O'Beirne[1], Josef P. Werne[1]

[1]Department of Geology and Environmental Science, University of Pittsburgh, Pittsburgh, PA, 15213, United States
[2]Lamont-Doherty Earth Observatory, Columbia University, Palisades, NY, 10964, United States
[3]Department of Earth, Geographic and Climate Sciences, University of Massachusetts Amherst, Amherst, MA, 01003, United States
[4]Department of Geography, Hong Kong Baptist University, Kowloon Tong, Hong Kong
[5]Department of Geological Sciences, State University of New York, Binghamton, NY 13902, United States
[6]Department of Geosciences, The University of Arizona, Tucson, AZ 85721, United States
[7]Department of Geological Sciences, University of Saskatchewan, Saskatoon, SK S7N 5E2, Canada

Correspondence to: Evan R. Collins (erc92@pitt.edu/ecollins452@gmail.com)

Abstract. The Methane Index (MI) is an organic geochemical index that uses isoprenoid glycerol dialkyl glycerol tetraethers (GDGTs) as a proxy for methane cycling. Here, we report results from sediments in core MAG14-2A that span almost 500 ka in Lake Magadi, Kenya. The deposits show abrupt shifts between high and low MI values through calcareous, tuffaceous and zeolitic silts. The MI "switches "off" (MI < 0.2), and "on" (MI > 0.5) through the core with bulk organic matter enriched in ^{13}C during "MI-off" periods (~ -18‰) in the upper part of the core, whereas ^{13}C is lower (-22 to -25‰) in lower parts of the sedimentary sequence. Sediments deposited when the MI switches "on" showed $\delta^{13}C_{OM}$ values as low as -89.4 ‰, but most were within the range of -28 to -30‰, which is consistent with contributions from methanogens rather than methanotrophs. Thus, the likely source of these high MI values in Lake Magadi is methanogenic archaea. Our results show that hydrothermal inputs of bicarbonate-rich waters into Lake Magadi combined with further evaporative concentration cause a shift in the dominant archaeal communities, alternating between two stable states.

1 Introduction

Life thrives in East African soda lakes and has been the subject of modern studies of both prokaryotic and eukaryotic organisms, but few have studied their sediments over geologic timescales (Schagerl, 2016 and

chapters therein). Soda lakes represent ~ 18,500 km^2 in East Africa (calculated from values in Melack
and MacIntyre, 2016). When compared to the three largest African freshwater lakes (lakes Victoria,
Tanganyika, and Malawi), these soda lakes account for ~ 13% of the total lake-surface area in East Africa.
A survey of microbial isolate diversity in East African lakes found evidence for cyanobacterial and
archaeal primary producers with both oxygenic and anoxygenic phototrophs among the microbial
population (Grant and Jones, 2016). Unique aerobic and anaerobic heterotrophs that use a variety of
electron donors, including sulfur, sulfate, nitrite, carbon dioxide, and methane, were also identified (Grant
and Jones, 2016, and sources therein). Many thermophilic archaea and bacteria isolates were also
observed near hot-spring outflows (Grant and Jones, 2016).

Saline alkaline (soda) lakes in the East African Rift often become stratified meromictic water bodies with
a dense monimolimnion below a chemocline (Melack and MacIntyre, 2016). Oxygen rarely penetrates
the monimolimnion waters, and as a result, anaerobic bacteria and archaea dominate the bottom waters
and sediments. Remineralizing organic matter from the upper water column (mixolimnion) supports the
microbes and ~~generation of~~the anaerobic oxidation of methane (AOM). Methane-oxidizing microbes,
specifically archaeal anaerobic methane-oxidizers (ANME), are coupled to sulfate-reducing bacteria in a
microbial consortium (Boetius et al., 2000; Hinrichs and Boetius, 2002; Werne et al., 2004). ANME
mediate methane levels in freshwater and soda lakes and in modern oceanic systems, and account for
approximately 90% of methane consumed through AOM (Egger et al., 2018). Rates of methane
consumption differ by environment and type of ANME, with global freshwater systems ranging from 1
to 1 x 10^5 nmol methane L^{-1} day^{-1} consumed (Martinez-Cruz et al., 2018). Although soda lakes have been
less studied, consumption rates as high as 1.6 x 10^4 nmol methane L^{-1} day^{-1} have been observed in
freshwater Lake Kivu (Roland et al., 2018). Tracking AOM over geologic time periods is important
because methane release from tropical wetlands was concomitant with the end of glacial conditions in
Europe and is poorly constrained (DeMenocal et al., 2000; Riddell-Young et al., 2023). Additionally,
large methane releases might have been partly responsible for the Permo-Triassic mass-extinction event
(Berner, 2002).

Over geologic time, it is possible to gauge periods of increased methane oxidation, as shown by Zhang et al. (2011) in oceanic systems by using a ratio of archaeal GDGT lipids (de Rosa et al., 1977; Langworthy, 1977). The ratio, as described by Zhang et al. (2011), is known as the methane index (MI), which uses GDGTs produced predominantly by Euryarchaeal ANME. The MI has been used to discern methanotrophy using the assumption that benthic methanotrophic Euryarchaeota preferentially produce GDGT-1, -2, and -3, and that GDGTs crenarchaeol (cren) and crenarchaeol′ (cren′) are thought to come from Thaumarchaeota and Crenarchaeota, which are part of the TACK superphylum, typically found in the upper water column (Sinninghe Damsté et al., 2002; Pitcher et al., 2009; Zhang et al., 2011). Currently, the newly suggested names in the Genome Taxonomy Database for Thaumarchaeota and Crenarchaeota are Nitrososphaerota and Thermoproteota, respectively (Oren and Garrity, 2021; Rinke et al., 2021), which are used in this paper.

Moreover, Kim and Zhang (2023) have shown a qualitative and quantitative relationship between the MI and methanotrophy in deep time, namely from the late Oligocene to the early Miocene. Kim and Zhang (2023) showed that the MI is applicable to AOM, with other biomarkers co-occurring in high-MI intervals representative of not only the Group I consortium of anaerobic methanotrophs (ANME) that produce GDGTs, but also of Group 2 and Group 3 consortia (ANME-2 and ANME-3 respectively). Until now, no studies have directly applied the MI to sediments in African soda lakes despite evidence for AOM in modern soda lakes. Combined with MI values, other methane-related indices are used here to interpret methanogenesis and methanotrophy related to AOM. Previous studies have used GDGT-0 and GDGT-2 ratioed to the GDGT crenarchaeol value, which was originally thought to only be produced by mesophilic Thermoproteota (Blaga et al., 2009; Weijers et al., 2012). However, the optimum temperature for crenarchaeol production is closer to 40-45 ºC (Zhang et al., 2006). Blaga et al. (2009) found that methanogens predominantly produced GDGT-0, whereas Weijers et al. (2011) showed that methanotrophic archaea predominantly produce GDGT-2. However, the optimum temperature is closer to 40-45 ºC (Zhang et al., 2006).

Lake Magadi (Kenya) is a sulfate-limited lake, and therefore, methanogenesis and methanotrophy may co-occur without suppression of the higher energy yield of sulfate reduction (Nijaguna, 2006; Sorokin et al., 2007; Deocampo and Renaut, 2016; Lameck et al., 2023). Here, we document evidence of methane cycling in Lake Magadi using archaeal isoprenoid GDGT lipid biomarkers. Environmental influences on archaeal community composition included precipitation/evaporation fluctuations and variations in hydrothermal activity, the latter often related to contemporary tectonics. This study leverages four methane-related indices: (1) the MI; (2) the %GDGT-0/crenarchaeol; (3) %GDGT-2/crenarchaeol; and (4) the ratio of isoprenoid GDGTs [2]/[3] (hereafter, [2]/[3]) to understand methane cycling in recent and ancient lacustrine sediments. Two distinct communities were found using a combination of the MI and ratios of GDGT-0 and GDGT-2, normalized to crenarchaeol. Intervals of high methanotrophy, as evidenced by MI and %GDGT-2/crenarchaeol, were related to an equally high proportion of methanogens, while in periods when crenarchaeol was dominant, the methane indices were low.

2   Materials and methods

2.1   Study locations and sampling

Modern Lake Magadi is a seasonally flooded, saline alkaline pan composed of bedded trona ($[Na_3(CO_3)(HCO_3) \cdot 2H_2O]$) located in the southern Kenya Rift near the border with Tanzania (Baker, 1958; Eugster, 1980). Its elevation is approximately 600–605 m above sea level (asl), and it has a maximum depth during the rainy season of a few decimeters to ~ 1 m (Fig. 1; Renaut and Owen, 2023). Although Lake Magadi is situated near the equator, it lies in a rain shadow. Consequently, today it has a large moisture deficit (2400 mm evaporation versus 500 mm precipitation annually: Damnati and Taieb, 1995).

The modern alkaline lake is fed by ephemeral streams and alkaline hot springs (up to 86°C at adjacent Nasikie Engida), distributed along faults around the shoreline (Baker, 1958; Crane, 1981; Allen et al., 1989; Renaut and Owen, 2023). Former high-level shorelines are preserved as coarse clastic sediments and locally as stromatolites around the lake. These vary in age and record lakes of different depths during

110 the Quaternary. Outcrops of sediments relevant to this study and situated near Lake Magadi are the Oloronga Beds and the Green Beds. The chert-bearing Oloronga Beds in outcrop ~~have been dated~~were lain down between ~ 800 and 300 ka, with cores extending this back to 1 Ma (Owen et al., 2019). Green Beds outcrops include abundant chert and have been variably dated between 191 and 40 ka (Behr and Röhricht, 2000; Owen et al., 2019) with cores suggesting a range from 380 to 105 ka (Owen et al., 2019).

115 ~~More recently, t~~The High Magadi Beds were deposited between ~25 and 9 ka (Fairhead et al., 1972; Goetz and Hillaire-Marcel, 1992; Williamson et al., 1993; Behr and Röhricht, 2000; Owen et al., 2019; Reinhardt et al., 2019). Calcrete commonly caps the Oloronga Beds (Eugster, 1980), but fluvial erosion locally scoured those sediments before the Green Beds were laid down (Renaut and Owen, 2023).

120 ~~More recently, the stratigraphic terminology has been revised by Owen et al. (2025). They continued to recognise the Oloronga Beds below Lake Magadi under the same name but raised it to formation status with dates of 1000–380 ka. In contrast, they renamed the Green Beds to the Oloika Formation (380–105 ka) and reassigned the Evaporite Series to the Magadi Formation (105–0 ka) and the High Magadi Beds to the High Magadi Formation. Various higher lake-levels have been suggested based on stromatolites~~
125 ~~(Casanova and Hillaire-Marcel, 1987) but some details are uncertain. Although Lake Magadi is situated near the equator, it lies in a rain shadow. Consequently, today it has a large moisture deficit (2400 mm evaporation versus 500 mm precipitation annually: Damnati and Taieb, 1995).~~

Lake Magadi was cored as part of the *Hominin Sites and Paleolakes Drilling Project* (HSPDP) in June
130 2014 to further our understanding of the paleoenvironments in the East African Rift Valley and to better contextualize hominin remains and artifacts, and to understand possible environmental influences on hominin evolution and migration (Cohen et al., 2016). A 197.4-meter core (MAG-14-2A) was drilled in the northern end of Lake Magadi (1°51'5.76" S 36°16'45.84" E; Owen et al., 2019). In total, 107.7 m of sediments were recovered, with an overall core recovery of 55.4% (Cohen et al., 2016). Here, we use the
135 age model from Owen et al. (2019). The core ranges from the modern trona surface (0 ka) to the Magadi Trachyte basement, dated to ~ 1 Ma at the core site (Owen et al., 2019). Cores were sampled in 2016 during the initial core description at the Continental Scientific Drilling Facility (CSD, formerly LacCore)

at the University of Minnesota, Minneapolis. Altogether, 61 samples, covering the period from 456 ka to 14.9 ka (Table S1), were collected and freeze-dried from dark brown to black silty clay intervals. Based on their color, these samples were expected to have a high total organic carbon that would yield the highest quantity of biomarkers for our study. The non-ideal sampling strategy is due to poor core recovery.

Over the past million years, Lake Magadi has varied from swampy fresh water bodies to a large fresh to mildly saline lake that was continuously fed by rivers and groundwater, to smaller hypersaline lakes bounded by the Magadi grabens that dried to trona pans partly fed by hot springs (Owen et al., 2019; Renaut and Owen, 2023). From 545 to 380 ka the Magadi catchment progressively changed to a more arid condition with the palaeolake marked by abundant calcareous, organic-rich sediments (Owen et al., 2019). Periodic freshwater inundation occurred from 380 to 105 ka into a highly saline, alkaline lake that accumulated minor calcite and magnesium-rich calcite at lake margins. Ash that fell into this waterbody reacted to form a variety of zeolites with anoxic, sulfate-rich bottom-water brines subjected to microbial sulfate reduction (Owen et al., 2019; Deocampo et al., 2022). The most recent phases of the lake (105 to 0 ka) were more evaporatively enriched, with abundant trona and minor nahcolite. Well-preserved diatoms in sediments deposited after ~500 ka suggest very high aqueous silica in the paleolake in order to explain the preservation of their frustules under highly alkaline conditions, which may reflect strong evaporative concentration of silica-rich hydrothermal inflows (Owen et al., 2019).

2.2 ~~Leaf wax~~GDGT and bulk organic preparation and analysis

2.2.1 Lipid extraction

To obtain a total lipid extract (TLE), 61 samples from Lake Magadi were freeze dried and homogenized and ca. 5–10 g of sediment were ultrasonically extracted with 2:1 DCM:MeOH. The TLE for each sample was treated with activated copper shot to remove elemental sulfur. The TLEs were then separated into three fractions (apolar (AP), polar one (P1), and polar two (P2)) using activated alumina via short column chromatography. The AP fraction was eluted with 4 mL of 9:1 Hexane (Hex):DCM (v/v), the P1 fraction with 4 ml 1:1 DCM:MeOH, and the P2 fraction with 4 ml MeOH. The P1 fractions were dried down and

165 re-dissolved in 99:1 Hex:Isopropanol (IPA) (v/v) and filtered through a 0.45 µm 4 mm diameter PTFE filter prior to GDGT analysis.

2.2.2   Bulk organic $\delta^{13}C_{OM}$ analysis

Samples were subsampled from the same intervals as organic biomarkers for bulk organic carbon isotope analysis. Powdered sediment samples were weighed in silver capsules and carbonates were removed by 170 adding 5% HCl in four-hour increments. Samples were analyzed on a Costech Elemental Analyzer coupled to a ThermoFinnigan Delta V Plus isotope ratio monitoring mass spectrometer (IRMS). Samples are reported as per mil (‰) deviations from the Vienna Pee Dee Belemnite (VPDB) standard in conventional delta notation.

2.3   GDGT preparation and analysis

175 ### 2.3.1   GDGT analysis

Polar samples from Lake Magadi were analyzed for core lipid isoprenoid glycerol dialkyl glycerol tetraethers (iso-GDGTs) at the University of Massachusetts Amherst on an Agilent 1260 series high performance liquid chromatograph (HPLC; Fig. S1) in tandem with an Agilent 6120 series single quadrupole mass selective detector (MSD). Compounds were ionized using atmospheric pressure 180 chemical ionization (APCI). The columns used for GDGT separation were a pre-column guard followed by two ultra-high performance liquid chromatography (UHPLC) silica columns (BEH HILIC, 2.1x150 mm, 1.7 µm, Waters) connected in series and kept at 30 °C. Elution solvents followed Hopmans et al. (2016) using a flow rate of 0.2 mL min^{-1}. Two solvent mixtures, hexane (A) and 9:1 Hex:IPA (B), were eluted isocratically for 25 minutes with 18% B, a linear gradient to 35% B in 25 minutes, a second linear 185 gradient to 100% B in 30 minutes.

2.3.2   GDGT indices

Several different ratios based on the relative abundance of different isoprenoid GDGTs have been developed to determine their source(s). The methane index (MI) is defined by Zhang et al. (2011) and is calculated as in Eq. (1):

190

$$MI = \frac{GDGT-1+GDGT-2+GDGT-3}{GDGT-1+GDGT-2+GDGT-3+Cren+Cren'} \qquad (1)$$

MI values range between 0 and 1 with values > 0.5 considered to be derived from methanotrophic communities and values < 0.3 considered normal sedimentary conditions (Zhang et al., 2011). These
195 proposed ranges from Zhang et al. (2011) were derived from GDGTs found in marine sediments, so the cutoff values for methanotrophy may differ in lacustrine sediments, particularly those in saline, alkaline environments.

The ratio of GDGT-2 / crenarchaeol (%GDGT-2/cren) also indicates methanotrophy (values > 0.2),
200 specifically methanotrophy associated with sulfate-methane transition zones (Weijers et al., 2011). These values were normalized and converted to percentages so that the numbers produced could be contextualized with the other indices used (Eq. 2). As a result, %GDGT-2/cren contributions greater than 33% will be considered methanotrophic signals.

205 $$\%GDGT - 2/cren = \frac{[GDGT-2]}{[GDGT-2]+[Cren]} * 100 \qquad (2)$$

Methanogenic inputs are calculated similarly to Eq. 2 above using GDGT-0 in place of GDGT-2. Blaga et al. (2009) found that values of GDGT-0 / (GDGT-0 + cren) > 2 are associated with methanogenic archaeal communities in a study of freshwater lakes. Similarly, in a study of Eocene marine sediments,
210 Inglis et al. (2015) normalized the equation and converted it to a percentage, a convention we follow (Eq. 3). They found that contributions from methanogens were indicated by values greater than 67%.

$$\%GDGT - 0/cren = \frac{[GDGT-0]}{[GDGT-0]+[Cren]} * 100 \qquad (3)$$

215 The GDGT-2 / GDGT-3 ([2]/[3]) index ~~was~~ is used here to describe both mesophilic environments as well as environments with high MI values. Rattanasriampaipong et al. (2022) found that differences in

[2]/[3] are linked to distinct archaeal communities whereby low values of [2]/[3] (ca. 0.55) are observed in thermophilic cultures while elevated values are indicative of hot spring mats (ca. 1.00), shallow aerobic ammonia-oxidizing archaea (AOA; ca. 1.16), or archaea in suspended particulate matter (ca. 2.52). This is the same version described in Rattanasriampaipong et al. (2022) (Eq. 4).

$$[2]/[3] = [GDGT-2]/[GDGT-3] \tag{4}$$

2.4   Bulk geochemistry

Bulk geochemical data and core descriptions from Owen et al. (2019, 2024) were used to interpret hot spring influences in the intervals of focus in the sediment core (designated as intervals 1, 3, and 5 in the results and discussion sections)~~intervals of focus (i.e., Intervals 1, 3, and 5)~~. They attributed rare earth element (REE) anomalies to increased lake alkalinity, which reflected increased evaporation and the development of highly saline, alkaline lakes and possibly increased hydrothermal/fluvial inflow ratios. All statistical analyses were performed using the GraphPad Prism 10$^{©}$ software (https://www.graphpad.com/). Only the necessary data to determine relationships between the bulk geochemistry of ~~rare earth elements~~REEs (~~REEs;~~ La, Ce, Nd, Sm, Eu, Yb, Lu) and methane indices (MI, %GDGT-0/cren, %GDGT-2/cren, and [2]/[3]) were imported. The data was tested for normality via the built-in "Normality and Lognormality Tests" function in Graph Pad$^{©}$. Tests yielded lognormal distributions of each dataset and found the data to be non-normally distributed. ~~Prior to performing a principal component analysis (PCA) or correlation matrix, the data needed to be tested for normality. To determine whether the data were normally distributed, the built-in "Normality and Lognormality Tests" function in GraphPad$^{©}$ yielded lognormal distributions of each dataset. The data were found to be non-normally distributed.~~Additionally, pyrite cubes were visually assessed without the use of a microscope during the initial core description and during organic extractions, however, no smear slides were collected and assessed.

2.4.1 Principal component analysis (PCA)

For the PCA, the imported data were analyzed using the built-in PCA function in GraphPad©. The data were standardized, which scaled the data to a mean of 0 and a standard deviation of 1. The principal components were selected based on their eigenvalues using the Kaiser Rule, which selects eigenvalues greater than 1.0. Principal components 1 and 2 explained 58.0% of the variance in the data.

2.4.2 Correlation matrix

The correlation matrix was performed using the built-in function in GraphPad©. Because the data were non-normally distributed, the nonparametric Spearman correlation was chosen over the Pearson correlation. An r value was computed for every pair of Y datasets using the default two-tailed option at a 95% confidence interval.

3 Results

3.1 GDGT lipid variability

Samples are split into six intervals (1-6) based partly on their fractional abundances of GDGT-0 and cren as well as their MI values: (1) 35.67 to 32.61 m; ca. 17.7 to 14.9 ka, (2) 67.81 to 43.51 m; ca. 129 to 38.9 ka (3) 86.06 to 70.78 m; ca. 197 to 149 ka, (4) 96.38 to 94.91 m; ca. 318 to 315 ka, (5) 104.10 to 103.16 m; ca. 324 to 323 ka, and (6) 130.21 to 119.64 m; ca. 456 to 391 ka (Table S1).

In each of the intervals of the core, ~~Table S1 Table S1~~MI, %GDGT-0/cren, and %GDGT-2/cren values oscillate between high and low values, changing abruptly from one interval to the next (Table S1). The methanotrophic (%GDGT-2/cren) and the methanogenic (%GDGT-0/cren) indices track similarly to MI values; that is, when values of MI are high, so are the other two indices. It should be noted that there are some large gaps in sampling between intervals in the core due to our sampling regime (i.e. targeting intervals with high apparent organic matter based on darker silty matrix). Interval 1 is characterized by a higher proportion of cren and lower overall index values. The %GDGT-0/cren index averages 36.3 % (±0.09 %) in this interval while the %GDGT-2/cren index averages 10.6 % (±0.05 %; Fig. 2). The MI in

this interval is correspondingly low with an average of 0.25 (±0.07), well below the MI = 0.5 cutoff range for methanotroph-impacted communities. As such, this interval could be used for the [2]/[3] index; values averaged 2.1 (±1.02). Interval 2 has much higher values for each of these indices, where the average %GDGT-0/cren = 99.3 % (±0 %) and the average %GDGT-2/cren = 93.6 % (±0.04 %). MI values in Interval 2 are also high with an average of 0.96 (±0.02). Of note, there is a large gap where no measurements were taken from 43.55 to 46.68~~15~~ m (~9.7 kyr) as well as from 50.36 to 58.74 m (~32.5 kyr). Interval 3 averages for %GDGT-0/~~/~~cren and %GDGT-2/cren are 54.3 (±0.27 %) and 20.4 % (±0.26 %), respectively. However, there is one anomalously high value at 77.32 m with %GDGT-0/cren and %GDGT-2/cren values at 99.6 and 93.8 % and an MI = 0.96. Excluding the high index value, the averages were lowered to 48.6 (±0.22%) and 11.2 % (±0.05%) for the %GDGT-0/cren and %GDGT-2/cren values and the MI average was lowered from 0.33 (±0.23) to 0.26 (±0.06). With the exclusion of 77.32 m, the [2]/[3] index averaged 1.5 (±0.80) in this interval, lower than Interval 1. Interval 4 is characterized by high index values, with a similarly abrupt shift from low values. Averages of the %GDGT-0/cren and %GDGT-2/cren are 98.1 (±0.04 %) and 88.2 % (±7.41 %) and an average MI of 0.92 (±0.04); these average index values are similarly high as compared to Interval 2. Interval 5 is a shift to lower overall index values with averages of %GDGT-0/cren and %GDGT-2/cren at 40.1 (±0.17 %) and 9.2 % (±0.03 %) and an average MI of 0.22 (±0.05). Finally, Interval 6 shows a period in the core with high index values throughout. Averages of %GDGT-0/cren, %GDGT-2/cren, and MI are 97.6 % (±0.03 %), 89.4 % (±0.08 %), and 0.95 (±0.05), respectively.

3.2 Bulk $\delta^{13}C_{OM}$ values

~~Table S1~~Bulk $\delta^{13}C_{OM}$ values follow a similar pattern to the indices described in section 3.1, that is the values oscillate between high and low values between intervals. Samples in Interval 1 ranged from -21.9 to -16.8 ‰ and had an average $\delta^{13}C_{OM}$ value of -18.4 ‰ with respect to VPDB. Interval 2 samples had the most ^{13}C-depleted values in all sampled intervals, ranging from -89.4 to -24.7 ‰ with an average of -35.1 ‰ and excluding the three outlier values (-48.1, -64.2, and -89.4 ‰), the Interval 2 average was -28.2 ‰. In Interval 3, the $\delta^{13}C_{OM}$ had a narrower range from -24.4 to -21.4 ‰ and an average of -22.5 ‰. A lighter signal from Interval 4 yielded a narrow range of values from -27.0 to -25.4 ‰ averaging -26.0

‰. Interval 5 had slightly heavier values ranging from -25.0 to -18.1 ‰ with an average of -22.1 ‰.

Lastly, Interval 6 had depleted $\delta^{13}C_{OM}$ values similar to intervals 2 and 4, with a range of -28.2 to -22.1 ‰ and an average of -25.2 ‰. Analytical reproducibility of duplicate runs was better than ± 0.15 ‰ VPDB.

3.3 Bulk geochemistry

Both a PCA and correlation matrix were performed using the MI, Ca/Na, %GDGT-0/cren, %GDGT-2/cren, and [2]/[3] to compare to the REEs La, Ce, Nd, Sm, Eu, Tb, Yb, and Lu (Fig. 3). Increased values of REEs are characteristic of sodic systems influenced by hydrothermal springs, ~~namely~~ such as Mono Lake in California and this system (Johannesson and Lyons, 1994; Owen et al., 2019). Additionally, the Ca/Na is a proxy for the proportion of hydrothermal inflow to Lake Magadi such that a higher Ca/Na indicates more freshwater input, while a lower Ca/Na indicates a higher proportion of hydrothermal water.

A PCA (Fig. 4a) and non-parametric Spearman correlation matrix (Fig. 4b) were performed to quantify the relationship between REEs, MI, Ca/Na and [2]/[3]. The PCA showed that Ca/Na loaded positively on PC1 and PC2 and each of the methane indices loaded positively on PC1 and negatively on PC2. The REE La loaded positively on PC2 and negatively on PC1 while the REEs Ce, Nd, Sm, Eu, Yb, and Lu loaded negatively on PCs 1 and 2. This indicates a negative relationship between the negatively loaded REEs and a high Ca/Na. Similarly, the correlation matrix of REEs and methane indices showed a negative relationship between each index and REE, except for the relationship of [2]/[3] and Nd (r=0.02) and %GDGT-2/crem (r=-0.04), which showed no observable linear trend. The REEs and methane indices did not load on the same PC axis showing that there was also not a nonlinear trend associated with the REEs and methane indices.

4 Discussion

4.1 Lake Magadi archaeal community shifts

The abrupt changes in isoprenoid GDGT-based indices in the sediment record of Lake Magadi indicate shifts in the archaeal communities present (Fig. 2). Shifts between two distinct communities were inferred

using a combination of the Methane Index (MI) and ratios of GDGT-0 and GDGT-2 normalized to crenarchaeol (Eqs. 2 and 3). We denote these shifts as either "MI-on periods", characterized by MI > 0.5 during intervals 2, 4, and 6, and "MI-off periods", characterized by MI < 0.5 during intervals 1, 3, and 5. Oscillations between these two states are discussed in detail in the following sections.

4.1.1   MI-on periods

In Lake Magadi, during the MI-on periods (Fig. 2; Intervals 2, 4, and 6), the MI is persistently greater than 0.83 and displays more ^{13}C-depleted $\delta^{13}C_{OM}$ values compared to MI-off periods, indicating periods of enhanced methane cycling. AOM is a likely mode of methane cycling in Interval 6 as well as parts of Interval 2 because SRB and AOM archaea live in a consortium together at the sulfate methane transition zone, or SMTZ (Boetius et al., 2000; Hinrichs and Boetius, 2002; Werne et al., 2004). Thus, in intervals of the Magadi core where a SMTZ is suspected, such as in parts of Interval 2 and most of Intervals 4 and 6, there should be an increase in indices related to methanotrophy such as high MI and %GDGT-2/cren (Weijers et al., 2011). Additionally, whereas methanogens and methanotrophs appear to be present in a consortium based on both the methane indices as well as bulk $\delta^{13}C_{OM}$, the majority of the contributions are coming from methanogens, as seen in the ternary plot in Fig. 5. This may seem counter-intuitive as the MI has been typically used to describe samples exhibiting a high predilection towards methanotrophy, but a high MI value does not necessarily exclude methanogenesis and conversely neither does a low MI, rather the low MI value suggests a predominance of Thermoproteota over Euryarchaeota (Zhang et al., 2011). High %GDGT-0/cren and %GDGT-2/cren index values in Intervals 2, 4, and 6 (Fig. 2) show that methanogenesis is co-occurring with AOM. The [2]/[3] index is also useful in understanding the proportion of methanotrophs in sediments, even in intervals with high MI values like those discussed herein (Table S1; Fig. 2). Values of the GDGT [2]/[3] ratio track nearly identically to the MI values (Fig. 2), indicating that the MI is influenced by GDGT-2, which is characteristic of methanotrophs (Pancost et al., 2001; Schouten et al., 2003; Zhang et al., 2011).

Typically, methanogenesis in sulfate-rich systems is suppressed in favor of sulfate reduction caused by competition for both H_2 and organic substrates (Fazi et al., 2021; Sorokin et al., 2015). However, reports

of methanogenesis co-occurring with SRB have been noted when methanogens are using non-competitive substrates such as methanol, or when sulfate levels are low (Oremland et al., 1982; Giani et al., 1984 Hoehler et al., 2001; Bebout et al., 2004; Arp et al., 2008, 2012; Jahnke et al., 2008; Smith et al., 2008;

350 Robertson et al., 2009). Furthermore, pyrite cubes are common and scattered through the intervals where high index values are observed, indicating that there was a substrate for SRB, though it may have been in low concentration (Table S1). Thus, the combined evidence of pyrite in intervals with high GDGT-based indices (e.g. MI, %GDGT-0/cren, and %GDGT-2/cren [2]/[3]) indicates the presence of a SMTZ that supports AOM with the co-occurrence of methanogenesis.

355

Looking at Figure 4̶5, it appears that GDGT-0 is the dominant GDGT compared to GDGT-2 and cren, indicating that this interval is likely methanogen-dominant rather than ANME dominant. Interval 2 (Figs. 3̶ 2 and 5) of the Magadi core appears to be more influenced by methanogenesis than AOM, ~~resulting from a more prevalent~~as seen in a high %GDGT-0/cren signal accompanied by a high %GDGT-2/cren

360 signal, high [2]/[3] ratios, and a more ^{13}C-depleted bulk $\delta^{13}C_{OM}$ signal (average = -35.1 ‰; median = -28.6 ‰). Values of bulk $\delta^{13}C_{OM}$ are similarly ^{13}C-depleted in AOM-dominant Euryarchaeotal systems ranging from active mud volcanoes (~-27 ‰; ANME-1), a Danish freshwater lake (average ~-29.7‰; ANME-2), and the Sea of Galilee (~-30 ‰; ANME-2) in Israel (Lee et al., 2018; Norði et al., 2013; Sivan et al., 2011). At points where the bulk $\delta^{13}C_{OM}$ values are at their lowest (e.g., -89 ‰), they are

365 accompanied by a lower %GDGT-2/cren at ca. 95 % and an elevated %GDGT-0/cren at > 99.5 %. This aligns with the literature as Summons et al. (1998) reported $\delta^{13}C_{OM}$ values between -53.4 and -48.7 ‰ in the total lipid extract of methylotrophic methanogens using non-competitive substrates in anoxic hypersaline environments. Furthermore, as these waters are typically sulfate-limited, acetoclastic and/or hydrogenotrophic methanogenesis is likely dominant when evidence for SRB is lacking (i.e., pyrite).

370 Zhuang et al. (2016) performed compound-specific isotope analysis on several archaeol compounds from the Orca Basin and found archaeol and hydroxyarchaeol using H_2 or CO_2 (diagnostic of methanogens and methanotrophs) were relatively depleted (ca. -80 to -60 ‰) compared to the bulk $^{13}C_{OM}$ (ca. -22 ‰). Zhuang et al. (2016) concluded that acetoclastic and/or hydrogenotrophic methanogenesis was unlikely due to high SO_4^{2-} concentrations in the Orca Basin, which may be the case in Lake Magadi. In Interval 2,

there is no evidence of visible pyrite cubes and we did not have a priority at the time of sampling to check a thin section of each sample for smaller pyrite aggregates. This indicates that other Euryarchaeotal communities may have different forms of AOM occurring in the sediments. These other forms of AOM include nitrate/nitrite reduction and iron coupled to AOM ('t Zandt et al., 2018). This is further bolstered by the evidence outlined by Kim and Zhang (2023) that not only quantitatively linked AOM to high MI values, but also to non-Group I ANME Euryarchaea because other non-GDGT producing ANME (e.g. ANME-2 and ANME-3) were shown to co-exist with Group I ANME. In the intervals that are missing pyrite (i.e., most of Interval 2; see Table S1; Ferland, 2017), the pyrite may have either been too small to see with the naked eye or the excess H_2S could have been incorporated into the kerogen by reacting with labile organic matter. From 59.40 to 58.80 m, values of the bulk $\delta^{13}C_{OM}$ dip as low as -89.4 ‰ (Table S1; Fig. 2), which aligns well with methanogenic archaeal biomass (Norði et al., 2013). However, as discussed above there is likely acetoclastic and/or hydrogenotrophic methanogenesis co-occurring in these high index intervals and is likely the dominant process where sulfate-dependent AOM is absent, and the sulfate-dependent AOM is likely replaced by coupling to either nitrate/nitrite or iron reduction.

Samples in Interval 4 (Table S1) of the Magadi core have high index values but no evidence for sulfate-dependent methanotrophy except for high MI values. This interval is thus interpreted as being methanogenic rather than methanotrophic. The abundance of pyrite in the four samples with low MI values (Table S1; 104.10 to 103.16 m), indicates sulfate reduction not linked to AOM. This is not observed in any other level of the core and a hypothesized series of reactions is described below, which may be linked to an abundance of SRB, anaerobic ammonium oxidizing (anammox) bacteria, and Thermoproteota (AOA) in the overlying water column. Due to periodic influxes of freshwater in Magadi, in addition to a permanent meromixis present in almost all samples in this study post 380 ka, the water column would have been oxic in the upper portion and anoxic below the chemocline. Freshwater pulses would have also brought nutrients to the lake such as ammonia (NH_4^+) and sulfate (SO_4^{2-}). The oxic portion of the water column would have supported microaerophilic AOA that oxidize NH_4^+ to nitrite (NO_2^-), which is then transported to the anoxic part of the water column (Straka et al., 2019). Here, anammox bacteria use excess NH_4^+ and NO_2^- from the AOA and convert these to N_2. Excess SO_4^{2-} is

simultaneously being used by SRB, creating HS⁻ that is reacting with iron species in the sediments and being buried as pyrite. Ladderane lipids characteristic of marine annamox bacteria (Jetten et al., 2009) were not studied in Magadi sediments. However, there is both 16S rRNA and lipid evidence for the production of ladderanes in hot springs in the western United States suggesting that annamox bacteria can persist in hot spring environments (Jaeschke et al., 2009). Additionally, Kambura et al. (2016) found evidence for *Planctomycetes* in both microbial mat and water samples surrounding the hot springs of Lake Magadi, lending credence to the hypothesis of AOA persisting in Lake Magadi. Without other lines of evidence, however, these are hypothetical reactions for explaining excess pyrite in the sediments without accompanying MI values. Nonetheless, this explanation has merit because of the high relative abundance of both crenarchaeol and cren′.

In nearly all of Interval 6 (Table S1), there is evidence for a higher proportion of methanotrophic archaea from 128.74 to 119.64 m (increased %GDGT-2/cren and [2]/[3]) and methanogenesis in the intervals from 130.21 to 129.77 m (Table S1; higher %GDGT-0/cren compared to %GDGT-2/cren). Samples from 123.43 to 119.64 (Table S1) are of note because the [2]/[3] values are lower than the MI values whereas every other MI and [2]/[3] values align nearly 1:1. This is likely due to GDGT-2 not being the dominant control of the MI. ~~and w~~While both %GDGT-0/cren and %GDGT-2/cren are equally high, there may be other factors in the water column exporting GDGT-2 to the sediments, possibly from deep-dwelling Group I.1b Thermoproteota, although this is unlikely due to limitations of depth (Taylor et al., 2013). The 656 m paleoshoreline reported by Casanova (1986, 1987) and Casanova and Hillaire-Marcel (1987) would imply a maximum water depth of ~ 50 m during the Late Pleistocene (African Humid Period: AHP) based on present topography. However, sedimentary evidence for such a high paleoshoreline is not seen throughout the Magadi Basin. Earlier water depths are also unclear because accommodation space was changing as the axial rift developed with faulting and subsidence (Owen et al., 2024). This is not deep enough (> 1 km) to support Group I.1b Thermoproteota per the constraints outlined in Taylor et al. (2013).

4.1.2 MI-off periods

In intervals characterized by low MI, %GDGT-0/cren and %GDGT-2/cren values (Fig. 2; MI-off intervals are odd numbers highlighted in blue), the $\delta^{13}C_{OM}$ values are ^{13}C-enriched relative to those intervals characterized by higher index values (Fig. 2; MI-on; Fig. 2). Since the methane cycling indices (%GDGT-0/cren and %GDGT-2/cren) are both predominantly influenced by the availability of crenarchaeol, MI-off periods are marked by increased production in crenarchaeol. Typically, crenarchaeol is produced in open ocean systems, freshwater lakes, and soils by the mesotrophic aerobic ammonium oxidizing phylum Nitrososphaerota. However, they can also be found in other environments, such as in hot spring mats in made by Thermoproteota (Pearson et al., 2004, 2008; Schouten et al., 2013). As Thermoproteota require oxygen to oxidize ammonium to nitrate, the increased presence of crenarchaeol in the MI-off intervals, therefore, suggests periods when conditions were more oxic, at least in the upper water column. The increase in crenarchaeol, as well as the low [2]/[3] index values, suggest that more Thermoproteota were present in Lake Magadi in those periods. As mentioned in Section 4.1.1, three groups of AOA are of interest for interpreting which archaeal groups are found in low index intervals of Lake Magadi. Averages of [2]/[3] from the global dataset in Rattanasriampaipong et al. (2022) are as follows: hot spring mats (avg. = 1.00), shallow AOA cultures (avg. = 1.16), and shallow core tops (avg. = 2.64). Placing these on a continuum, we can approximate the environment from [2]/[3] averages in Magadi, though it should be noted that the shallow AOA and shallow core-top values in Rattanasriampaipong et al. (2022) are based on marine core-tops, while the hot spring mats are based on terrestrial hot springs like those observed around Lake Magadi (i.e. pH > 6.5).

Interval 1 captures a transition from a more arid East Africa to a wetter period at the onset of the African Humid Period (AHP). During wetter periods, more allochthonous material is transported to the lake, which includes vegetal remains that impact the overall bulk $\delta^{13}C_{OM}$ values. This allochthonous vegetation enriches the overall bulk $\delta^{13}C_{OM}$ values more significantly than other intervals in the Magadi core. Average values of bulk $\delta^{13}C_{OM}$ are -17.7 ‰ in Interval 1, which correspond to the $\delta^{13}C_{OM}$ values of aquatic sedges mixed with a terrestrial signal of grassy woodland (Sikes, 1994; Reiffarth et al., 2016).

Pollen records in Lake Magadi indicate that a mixture of C4 grassy woodlands and C4 aquatic sedges were predominant in the landscape that surrounded Lake Magadi at this time (Muiruri et al., 2021). In agreement with the pollen record, the $\delta^{13}C_{OM}$ values likely record a mixture of C4 grasses and C4 sedges. Similar $\delta^{13}C$ values were reported in C_{21} to C_{33} n-alkanes in equatorial regions of Cameroon, ranging from -18.2 to -17.6‰ and recording the signals from C4 grasses and sedges (Garcin et al., 2014). ~~Supporting the pollen record, the $\delta^{13}C_{OM}$ values are likely reflecting $\delta^{13}C$ values similar to those observed by Garcin et al. (2014) in equatorial regions of Cameroon. The bulk $\delta^{13}C_{OM}$ is likely recording a mixture of C4 grasses and C4 sedges similar to $\delta^{13}C$ values of C_{27} to C_{33} n-alkanes obtained from C4 grasses and sedges in Cameroon which ranged from -18.2 to -17.6 ‰ (Garcin et al., 2014).~~ This all suggests that the bulk $\delta^{13}C_{OM}$ signal is dominated by terrestrial biomass, unlike other sections of the core, and there does not appear to be a significant influence from the benthic microbial community (i.e., methane cyclers or SRB).

Values of the [2]/[3] index average 2.1 in Interval 1 with some values as high as 3.74 and 4.63 at 33.28 and 33.03 m, respectively (Table S1). The higher values are closer to what is captured from deep oceanic suspended particulate matter (SPM) and deep ocean core-tops below the pycnocline, though caution should be used when comparing lacustrine and oceanic sediments (Rattanasriampaipong et al., 2022). The increase in %GDGT-0/cren (50.6 and 54.3 %; Table S1) and the slightly increased MI values (0.37 and 0.41; Table S1) imply that these samples were deposited in a deeper lacustrine environment. Evidence for a deeper paleolake at ~40 feet (~17–18 m) above the modern lakeshore (Baker, 1958) is also observed in the High Magadi Formation (ca. 17.7 to 10.8 ka) indicating that there was fresh water flowing into the lake during the period of deposition in Interval 1, likely creating a fresher water cap on the meromictic Lake Magadi (Barker et al., 1991; Behr, 2002; Owen et al., 2019). However, excluding the high [2]/[3] index values in Interval 1, the average is 1.6, which is closer to the hot spring mats and shallow AOA cultures (Rattanasriampaipong et al., 2022). Likely, the higher [2]/[3] index values represent periods of increased methanogenesis occurring in the sediments, with AOA input from the upper water column likely induced by proportional increases in the amount of hydrothermal inflow to the lake (Section 4.2.1). Fig. 4 shows that the Ca/Na is anti-correlated with REEs in both the PCA and correlation matrix. Since the

proportion of Ca/Na decreases when REEs increase, we can say that statistically, when it is drier (and thus proportionately more hydrothermally influenced) the Ca/Na decreases, REE values increase, and the methane indices are suppressed. In the periods of lower [2]/[3] values, the community is interpreted as being dominated by AOA and thermophilic AOA cultures (i.e., Thermoproteota; Rattanasriampaipong et al., 2022) and is further supported by high % cren and % cren′. Kumar et al. (2019) described similarly low [2]/[3] values in the water column of Lake Malawi that are akin to values observed in Lake Magadi in both Intervals 1 and 3. They found that values of a lower normalized [2] / [2+3], ranging from 0.55 to 0.59, in Lake Malawi were associated with the shallower Thermoproteota (Thaumarchaeota) Group I.1b. This is compared to higher values of [2] / [2+3] in the deeper dwelling Thermoproteota Group I.1a, which means that most samples in Interval 1 are likely sourced from Group I.1b (Kumar et al., 2019). Kumar et al. (2019) concluded that Group I.1b Thermoproteota were contributing to the lower [2] / [2+3] values, while the more deeply dwelling Group I.1a Thermoproteota were more prevalent in aphotic portions of the water column (Kumar et al., 2019). The normalized [2] / [2+3] used by Kumar et al. (2019), with values ranging from 0.55 to 0.65, approximates values of [2]/[3] in the 1.30 to 1.65 range as described in this paper. More recently, Baxter et al. (2021) found that Thermoproteota I.1b are more prevalent in the upper oxygenated portion of the water column within the photic zone as evidenced by a higher relative abundance of crenarchaeol and lower relative abundance of GDGT-2. Thus, our interpretations of thaumarcheotal AOA in Lake Magadi sediments are consistent with data from Baxter et al. (2021) and Kumar et al. (2019). This interpretation is consistent with Interval 1 being a period of proportionately more freshwater and HCO_3^--rich hydrothermal input and a deeper lake overall, which would explain the accompanying increase in crenarchaeol.

Interval 3 [2]/[3] averages are lower overall (Table S1; avg. = 5.4), with only one outlying high value (ca. 77.32 m at a value of 36.7). Excluding this high index value, the [2]/[3] average drops to 1.5, which is closer to what is observed in shallow AOA cultures and hot spring mats. With most samples being closer to unity (i.e., [2]/[3] = 1.0), it is likely that hot springs had a greater influence on the community composition in these intervals. Samples that are closer to unity (70.78, 70.86, and 71.08 to 75.93 m) also have a relatively ^{13}C-enriched $\delta^{13}C_{OM}$ values (avg. = -21.8‰) compared to samples with a higher [2]/[3].

(averaging 1.5 excluding the outlying value of 36.7). This average is closer to shallow Group I.1a Thermoproteota as described previously. Average isotope values in Interval 3 are between oceanic hydrothermal vents (avg. = -19.0 ‰) and terrestrial alkaline hot spring systems such as the Bison Pool

515 hot spring in Yellowstone National Park (avg. = -24.9 ‰) (Shah et al., 2008; Schubotz et al., 2013). Since elevated amounts of GDGT-2 (i.e., relative abundance > 45%) are associated with Euryarchaeota, and values in Intervals 1, 3, and 5 are much lower than 45% (Table S1), these intervals are likely dominated by Thermoproteotal AOA (Pancost et al., 2001; Turich et al., 2007; Taylor et al., 2013). Archaeal community composition in Intervals 1, 3, and 5 is independent of these external factors and is related to

520 hydrothermal flows. This further supports the hot springs driving the lake archaeal community composition as there was less overall precipitation and the Thermoproteotal communities were more abundant during Intervals 1, 3, and 5.

Lastly, Interval 5, which only has 4 samples, has similarly low values of [2]/[3] (average = 1.4) like

525 Intervals 1 and 3, which is likely indicative of Thermoproteotal AOA cultures. The CPI$_{alk}$ and CPI$_{FA}$ averages were 4.6 and 5.0, indicating more terrestrial input. So, while these values are lower than Interval 3, and closer to the values in Interval 1, these still indicate a higher terrestrial input during this timeframe.

4.2 The influence of hot spring/runoff ratios on the archaeal methane cycles

Hydrothermal fluids in the basin are rich in carbonate and bicarbonate as well as Na$^+$ ions, inferred to be

530 a result of the weathering and alteration of trachytic (silica-rich) basement rock (Jones et al., 1977; Allen et al., 1989), and mantle-derived CO_2 discharged mainly along faults (Lee et al., 2017; Muirhead et al.). Ca^{2+} and Mg^{2+} are also very low (Deocampo and Renaut, 2016). Renaut and Owen (2023) note that hydrothermal waters become important contributors to lake recharge during arid phases when fluvial inflow declines. For example, Nasikie Engida, a small hypersaline lake northwest of Lake Magadi, is

535 partly maintained today by hydrothermal inputs, with trona, nahcolite and zeolites accumulating during dry periods when there is little or no fluvial inflow (DeCort et al., 2019; Renaut et al., 2020; Renaut and Owen, 2023). Magadi Core MAG14-2A lacks evidence for complete desiccation (e.g., mudcracks, soils, calcrete) and the lake appears to have retained surface waters through multiple drought episodes during

the last million years (Owen et al., 2019). In contrast, separate lakes in the neighbouring Koora Basin (~10 km to the east), dried out many times, leading to soil formation in that basin (Owen et al., 2024).

Owen et al. (2019) also noted that during periods when highly saline, alkaline water dominated at Magadi, ash was zeolitized, REE patterns developed significant anomalies, and pyrite developed in anoxic/euxinic bottom waters of a meromictic lake. They also noted the excellent preservation of diatom opaline silica in highly alkaline lakes after about 540 ka, which suggests that very high levels of silica in lake water preserved their frustules from dissolution. Hydrothermal springs at Magadi today contain high silica, but their waters require further evaporation to achieve concentrations that would preserve diatom silica under very high pH conditions. High silica concentrations brought about by strong evaporation in a lake maintained by spring inflows (meteoric or hydrothermal) may partly explain the abundant chert through the Magadi sedimentary sequence.

Proportional increases in hot-spring water during periods of increased aridity would have favoured the development of highly saline, alkaline waters with significant impacts on archaeal communities. Samples in Interval 6 represent a drier period when the lake area and volume had shrunk, partly due to tectonic influences (Owen et al., 2024), and lake floor anoxia was prevalent (Owen et al., 2019). Between ~380 and 105 ka (Fig. 2; Interval 5 through mid-Interval 2), the paleolake was frequently meromictic with a freshwater mixolimnion that supported freshwater planktonic diatoms while the saline monimolimnion and lake floor waters favoured alteration of ash to a variety of zeolites (e.g., erionite, phillipsite, clinoptilolite, analcime) (Owen et al., 2019). Similarly, from ~105 to 0 ka (Fig. 2; mid-Interval 2 through Interval 1) low Ca/Na, increased Br, and the abundant zeolite formation, indicates saline conditions. After about 80 ka, tectonic adjustments and increasing aridity led to desiccation in the Koora Basin suggesting that spring inflows were important in maintaining a hypersaline lake in the Magadi Basin, as they do today during dry seasons (Owen et al., 2019). Ca/Na ratios have steadily decreased over time, though not at a 1:1 rate, which aligns with methane index values and sudden increases of these indices. Fig. 4 shows that the Ca/Na and methane indices are statistically different from one another in both the correlation matrix and PCA plot. In Fig. 5b4b, Ca/Na is loaded positively on PC1 and PC2, while the

methane indices ([2]/[3], MI, %0/Cren, and %2/Cren) are loaded positively on PC1 and negatively on PC2. Furthermore, REE data also appear to reflect our MI-off and MI-on periods as the REEs are anticorrelated in the correlation matrix (Fig. 5a4b) and loaded on different PC axes (Fig. 5b4a). Consequently, we interpret the changes in salinity and alkalinity in the Magadi paleolakes as reflecting the impact of climate on spring/runoff ratios into the Magadi Basin, which in turn have exerted significant impact on the archaeal communities through the last million years. Samples in the low-MI intervals (ca. 32.61–35.67, 70.78–75.93, and 103.2–104.1 m) likely reflect proportionally increased spring/-runoff ratios at Magadi caused by increased evaporation and decreased precipitation in the surrounding landscape.

5. Conclusions

Sediments in Lake Magadi track the environmentally driven changes in archaeal communities over the past ~ 456 ka. Using the MI to track the predominantly archaeal inputs at Lake Magadi, we have observed sudden and distinct shifts between mixed communities of Euryarchaeotal methanogens and methanotrophs transitioning to mesophilic AOA Thermoproteota communities and back again. This shift is driven, in part, by moisture balances in the East African Rift, with wetter conditions periodically causing freshwater floods into a saline lake to form a meromictic waterbody at Magadi, and with more archaea derived from the upper water column rather than the sediments, as evidenced by low MI, low [2]/[3], and relatively ^{13}C-enriched bulk $\delta^{13}C_{OM}$. Methane indices were typically higher during periods of reduced hydrothermal activity, indicating more Euryarchaeal communities, whereas Thermoproteota communities thrived during periods of higher hydrothermal activity. This is a clear relationship between low MI values, spring/runoff ratios, lake salinity, alkalinity and the development of mesophilic Thermoproteota. This study is one of the first to examine methane cycling in a soda lake over geologic time and provides valuable insights into how variable these systems can be. Soda lakes are important ecosystems for methane cyclers and should be studied more closely so that we can improve understanding of global methane contributions in the past, and constrain sources in the future.

6. Acknowledgements

We thank the Kenya National Council for Science and Technology (NCSTI) for granting research permits. Drilling and environmental permits were provided by the Kenya Ministry of Petroleum Mining and the National Environmental Management Authority of Kenya. We especially thank the National Environment Management Authority (NEMA). The Research Grants Council of Hong Kong provided support to RBORichard Bernhart Owen. We give special thanks the local Magadi Township Maasai community for their approval of the project and Tata Chemicals Magadi for providing , who provided field support. DOSECC Exploration Services supervised drilling that was undertaken by Drilling and Prospecting International (DPI). We also thank the CSDF facilities (University of Minnesota) for allowing us to store and log our cores at their repository. Drilling at Magadi for the Hominin Sites and Paleolakes Drilling Project (HSPDP) was funded by ICDP and NSF grants (EAR-1123942, BCS-1241859, EAR-1338553). This is Publication #XXX of the Hominin Sites and Paleolakes Drilling Project.

REFERENCES

Allen, D. J., Darling, W. G., and Burgess, W. G.: Geothermics and hydrogeology of the southern part of the Kenya Rift Valley with emphasis on the Magadi-Nakuru area, Brit. Geol. Surv. Res. Rep., SD/89/1, 1989.

Arp, G., Ostertag-Henning, C., Yuecekent, S., Reitner, J., and Thiel, V.: Methane-related microbial gypsum calcitization in stromatolites of a marine evaporative setting (Münder Formation, Upper Jurassic, Hils Syncline, north Germany), Sedimentology, 55, 1227–1251, 2008.

Arp, G., Helms, G., Karlinska, K., Schumann, G., Reimer, A., Reitner, J., and Trichet, J.: Photosynthesis versus exopolymer degradation in the formation of microbialites on the atoll of Kiritimati, Republic of Kiribati, Central Pacific, Geomicrobiol. J., 29, 29–65, 2012.

Baker, B.H.: Geology of the Magadi area, Geol. Surv. Kenya Rep., 42, 1958.

Barker, P., Gasse, F., Roberts, N., and Taieb, M.: Taphonomy and diagenesis in diatom assemblages; a Late Pleistocene palaeoecological study from Lake Magadi, Kenya, Hydrobiologia, 214, 267–272. 1991.

620 Bauersachs, T., Schwark, L.: Glycerol monoalkene diol diethers: a novel series of archaeal lipids detected in hydrothermal environments, Rapid Commun. Mass Sp., 30, 54–602016.

Baxter, A. J., Van Bree, L. G. J., Peterse, F., Hopmans, E. C., Villanueva, L., Verschuren, D., and Sinninghe Damsté, J. S.: Seasonal and multi-annual variation in the abundance of isoprenoid GDGT membrane lipids and their producers in the water column of a meromictic equatorial crater lake (Lake

625 Chala, East Africa), Quaternary Sci. Rev., 273, 107263, 2021.

Bebout, B. M., Hoehler, T. M., Thamdrup, B. O., Albert, D., Carpenter, S. P., Hogan, M., Turk, K., and Des Marais, D. J.: Methane production by microbial mats under low sulphate concentrations, Geobiology, 2, 87–96, 2004.

Behr, H. J., and Röhricht, C.: Record of seismotectonic events in siliceous cyanobacterial sediments

630 (Magadi cherts), Lake Magadi, Kenya, Int. J. Earth Sci., 89, 268–283, 2000.

Behr, H. J.: Magadiite and Magadi chert: a critical analysis of the silica sediments in the Lake Magadi Basin, Kenya, in Sedimentation in Continental Rifts (SEPM Spec. Publ. 73), edited by: Renaut, R.W., and Ashley, G.A., SEPM, Tulsa, 257–273, 2002.

Birgel, D., Meister, P., Lundberg, R., Horath, T. D., Bontognali, T. R., Bahniuk, A. M., de Rezende, C.

635 E., Vasconcelos, C., and McKenzie, J. A.: Methanogenesis produces strong ^{13}C enrichment in stromatolites of Lagoa Salgada, Brazil: a modern analogue for Palaeo-/Neoproterozoic stromatolites? Geobiology, 13, 245–266. 2015.

Blaga, C. I., Reichart, G. J., Heiri, O., and Sinninghe Damsté, J. S.: Tetraether membrane lipid distributions in water-column particulate matter and sediments: a study of 47 European lakes along a

640 north–south transect, J. Paleolimnol., 41, 523–540, 2009.

Bligh, E.G., and Dyer, W.J.: A rapid method of lipid extraction and purification, Can. J. Biochem. Phys. 37, 911–917, 1959.

Boetius, A., Ravenschlag, K., Schubert, C. J., Rickert, D., Widdel, F., Gieseke, A., Amann, R.

Jørgensen, B.B., Witte, U., and Pfannkuche, O.: A marine microbial consortium apparently mediating
645 anaerobic oxidation of methane, Nature, 407, 623–626, 2000.

Casanova., J.: Les Stromatolites Continentaux: Paléoécologie, Paléohydrologie, Paléoclimatologie.
Application au Rift Gregory, Thèse Docteur d'Etat-Sciences, Université d'Aix Marseille II, France,
1986.

Casanova, J.: Stromatolites et hauts niveaux lacustres Pléistocènes du basin Natron-Magadi
650 (Tanzanie-Kenya), Sci. Géol. Bull., 40, 135–153, 1987.

Casanova, J., Hillaire-Marcel, C.: Chronologie et paléohydrologie des hauts niveaux quaternaires du
basin Natron-Magadi (Tanzanie-Kenya) d'après la composition isotopique (^{18}O, ^{13}C, ^{14}C, U/Th) des
stromatolites littoraux, Sci. Géol. Bull., 40, 121–134, 1987.

Cassar, N., Laws, E. A., Bidigare, R. R., and Popp B. N.: Bicarbonate uptake by Southern Ocean
655 phytoplankton, Global Biogeochem. Cy., 18, GB2003, doi:10.1029/2003GB002116, 2004.

Castañeda, I. S., and Schouten, S.: A review of molecular organic proxies for examining modern
and ancient lacustrine environments, Quaternary Sci. Rev., 30, 2851–2891, 2011

Cohen, A., Campisano, C., Arrowsmith, R., Asrat, A., Behrensmeyer, A. K., Deino, A., Feibel,
C., Hill, A., Johnson, R., Kingston, J., Lamb, H., Lowenstein, T., Noren, A., Olago, D., Owen, R. B.,
660 Potts, R., Reed, K., Renaut, R., Schäbitz, F., Tiercelin, J.-J., Trauth, M. H., Wynn, J., Ivory, S., Brady,
K., O'Grady, R., Rodysill, J., Githiri, J., Russell, J., Foerster, V., Dommain, R., Rucina, S., Deocampo,
D., Russell, J., Billingsley, A., Beck, C., Dorenbeck, G., Dullo, L., Feary, D., Garello, D., Gromig, R.,
Johnson, T., Junginger, A., Karanja, M., Kimburi, E., Mbuthia, A., McCartney, T., McNulty, E.,
Muiruri, V., Nambiro, E., Negash, E. W., Njagi, D., Wilson, J. N., Rabideaux, N., Raub, T., Sier, M. J.,
665 Smith, P., Urban, J., Warren, M., Yadeta, M., Yost, C., and Zinaye, B.: The Hominin Sites and
Paleolakes Drilling Project: inferring the environmental context of human evolution from eastern
African rift lake deposits, Sci. Dril., 21, 1–16, https://doi.org/10.5194/sd-21-1-2016, 2016.

Crane, K.: Thermal variations in the Gregory Rift Valley of southern Kenya (?), Tectonophysics
74, 239–262, 1981.

670 Damnati., B., and Taieb, M.: Solar and ENSO signatures in laminated deposits from Lake Magadi (Kenya) during the Pleistocene/Holocene transition, J Afr. Earth Sci., 21, 373–382. https://doi.org/10.1016/0899-5362(95)00094-A, 1995.

DeMenocal, P., Ortiz, J., Guilderson, T., Adkins, J., Sarnthein, M., Baker, L., and Yarusinsky, M.: Abrupt onset and termination of the African Humid Period: rapid climate responses to gradual
675 insolation forcing, Quaternary Sci. Rev., 19, 347–361, 2000.

Deocampo, D. M., and Renaut, R. W.: Geochemistry of African soda lakes, in Soda Lakes of East Africa, edited by: Schagerl, M., Springer, Cham, 77–96, 2016.

Deocampo, D. M., Owen, R. B., Lowenstein, T. K., Renaut, R. W., Rabideaux, N. M., Billingsley, A., Cohen, A., Deino, A.L., Sier, M.J., Luo, S., Shen, C.-C., Gebregiorgis, D., Campisano, C., and Mbuthia,
680 A., Orbital control of Pleistocene euxinia in Lake Magadi, Kenya, Geology, 50, 42–47, 2022.

De Cort, G., Mees, F., Renaut, R. W., Sinnesael, M., Van der Meeren, T., Goderis, S., Keppens, E., Mbuthia, A., and Verschuren, D.: Late-Holocene sedimentation and sodium carbonate deposition in hypersaline, alkaline Nasikie Engida, southern Kenya Rift Valley, J. Paleolimnol., 62, 279–300. 2019.

de Rosa, M., de Rosa, S., Gambacorta, A., Minale, L., and Bu'lock, J. D.: Chemical structure of the
685 ether lipids of thermophilic acidophilic bacteria of the *Caldariella* group, Phytochemistry, 16, 1961–1965, 1977.

Eugster, H. P.: Inorganic bedded cherts from the Magadi area, Kenya, Contrib. Mineral. Petrol., 22, 1–31, 1969.

Eugster, H.P.: Chemistry and origin of the brines of Lake Magadi, Kenya, Mineral. Soc. Am. Spec.
690 Pap., 3, 213–235, 1970.

Eugster, H.P.: Lake Magadi, Kenya and its precursors, in Hypersaline Brines and Evaporites, edited by Nissenbaum, A., Elsevier, Amsterdam, 195–232, 1980.

Eugster, H.P., and Hardie, L.A., Saline lakes, in Lakes: Chemistry, Geology, Physics, edited by: Lerman, A., Springer, New York, 237–293, 1978.

695 Eugster, H.P.: Lake Magadi, Kenya: a model for rift valley hydrochemistry and sedimentation, in Sedimentation in the African Rifts (Geol. Soc. Lond. Special Publ. 25), edited by: Frostick, L.E., Renaut, R.W., Reid, I., Tiercelin, J.-J., 177–189, 1986.

Fairhead, J. D., Mitchell, J. G., and Williams, L. A. J.: New K/Ar Determinations on rift volcanics of S. Kenya and their bearing on age of rift faulting, Nature Phy. Sci., 238, 66–69, https://doi.org/10.1038/physci238066a0, 1972.

Fazi, S., Amalfitano, S., Venturi, S., Pacini, N., Vazquez, E., Olaka, L. A., Tassi, F., Crognale, S., Herzsprung, P., Lechtenfeld, O.J., Cabassi, J., Capecchiacci, F., Rossetti, S., Yakimov, M.M., Vaselli, O., Harper, D.M., and Butturini, A.: High concentrations of dissolved biogenic methane associated with cyanobacterial blooms in East African lake surface water, Commun. Biol., 4, 845, 2021.

Ferland, T., An Evaluation of the Organic Geochemical Potential to Reconstruct Mid-Pleistocene Paleoclimate Adjacent to an Established Hominin Site: Lake Magadi, Kenya (Doctoral dissertation, University of Pittsburgh), 2017.

Freeman, K. H., and Pancost, R.D.: Biomarkers for terrestrial plants and climate, in Treatise on Geochemistry, Volume 12, Second Edition, edited by: Holland, H.D., and Turekian, K.K., Elsevier, Amsterdam, 395–416, 2014.

Gallois, R. W., and Cox, B. M., The stratigraphy of the Lower Kimmeridge Clay of eastern England, Proc. Yorks. Geol. Soc., 41, 13–26, 1976.

Giani, D., Giani, L., Cohen, Y., and Krumbein, W. E. (1984). Methanogenesis in the hypersaline Solar Lake (Sinai), FEMS Microbiol. Lett., 25, 219–224.

Goetz, C., and Hillaire-Marcel, C., U-series disequilibria in early diagenetic minerals from Lake Magadi sediments, Kenya: dating potential, Geochim. Cosmochim. Acta, 56, 1331–1341. 1992.

Grant, W. D., and Jones, B. E., Bacteria, archaea and viruses of soda lakes, in Soda Lakes of East Africa, edited by: Schagerl, M., Springer, Cham, 97-147, 2016.

Hardie, L.A., and Eugster, H.P.: The evolution of closed-basin brines, Mineral. Soc. Am. Spec. Publ. 3, 273–290, 1970.

Hinrichs K.-U., and Boetius, A.: The anaerobic oxidation of methane: New insights in microbial ecology and biogeochemistry, in Ocean Margin Systems, edited by: Wefer, G., Billett, D. Hebbeln, D., Jorgensen, B.B., M. Schlüter, M. T., and van Weering, M.T., Springer, Berlin, Heidelberg, 457–477, 2002.

Hoehler, T. M., Alperin, M. J., Albert, D. B., and Martens, C. S.: Apparent minimum free energy

requirements for methanogenic Archaea and sulfate-reducing bacteria in an anoxic marine sediment, FEMS Microbiol. Ecol., 38, 33–41, 2001.

Hopmans, E. C., Schouten, S., and Sinninghe Damsté, J. S.: The effect of improved chromatography on GDGT-based palaeoproxies, Org. Geochem., 93, 1–6, 2016.

730 Inglis, G. N., Farnsworth, A., Lunt, D., Foster, G. L., Hollis, C.J., Pagani, M., Jardine, P. E., Pearson, P. N., Markwick, P., Galsworthy, A. M. J., Raynham, L., Taylor, K.W,R., and Pancost, R.D.: Descent toward the Icehouse: Eocene sea surface cooling inferred from GDGT distributions, Paleoceanography, 30, 1000–1020, https://doi.org/10.1002/2014PA002723, 2015.

In 't Zandt, M. H., de Jong, A. E., Slomp, C. P., and Jetten, M. S.: The hunt for the most-wanted 735 chemolithoautotrophic spookmicrobes, FEMS Microbiol. Ecol., 94, fiy064, 2018.

Jaeschke, A., Op den Camp, H. J., Harhangi, H., Klimiuk, A., Hopmans, E. C., Jetten, M. S., Schouten, S., and Sinninghe Damsté, J.S.: 16S rRNA gene and lipid biomarker evidence for anaerobic ammonium-oxidizing bacteria (anammox) in California and Nevada hot springs, FEMS Microbiol. Ecol., 67, 343–350, 2009.

740 Jahnke, L. L., Orphan, V. J., Embaye, T., Turk, K. A., Kubo, M. D., Summons, R. E., and Des Marais, D.J.: Lipid biomarker and phylogenetic analyses to reveal archaeal biodiversity and distribution in hypersaline microbial mat and underlying sediment, Geobiology, 6, 394–410, 2008.

Jetten, M. S., Niftrik, L. V., Strous, M., Kartal, B., Keltjens, J. T., and Op den Camp, H. J.: Biochemistry and molecular biology of anammox bacteria, Crit. Rev. Biochem. Mol. Biol., 44, 65–84, 745 2009.

Johannesson, K. H., & Lyons, W. B. (1994). The rare earth element geochemistry of Mono Lake water and the importance of carbonate complexing. Limnology and Oceanography, 39(5), 1141-1154.

Johnson, M. S., Matthews, E., Du, J., Genovese, V., and Bastviken, D.: Methane emission from global lakes: New spatiotemporal data and observation-driven modeling of methane dynamics indicates 750 lower emissions, J. Geophys. Res. Biogeosci., 127, e2022JG006793, 2022.

Jones, B.J., Eugster, H.P., and Rettig, S.F.: Hydrochemistry of the Lake Magadi basin, Kenya, Geochim. Cosmochim. Acta 41, 53–72, 1977

Kambura, A. K., Mwirichia, R. K., Kasili, R. W., Karanja, E. N., Makonde, H. M., and Boga, H. I.:

Bacteria and Archaea diversity within the hot springs of Lake Magadi and Little Magadi in Kenya,

755   BMC Microbiol., 16, 136, https://doi.org/10.1186/s12866-016-0748-x, 2016.

Kim, J. H., Van der Meer, J., Schouten, S., Helmke, P., Willmott, V., Sangiorgi, F., Koç, N., Hopmans, E.C., and Sinninghe Damsté, J. S.S.: New indices and calibrations derived from the distribution of crenarchaeal isoprenoid tetraether lipids: Implications for past sea surface temperature reconstructions, Geochim. Cosmochim. Acta, 74, 4639–4654, 2010.

760   Kim, B., and Zhang, Y. G.: Methane Index: Towards a quantitative archaeal lipid biomarker proxy for reconstructing marine sedimentary methane fluxes, Geochim. Cosmochim. Acta, 354, 74–87, 2023.

Knappy, C.S., and Keely, B.J: Novel glycerol dialkanol triols in sediments: transformation products of glycerol dibiphytanyl glycerol tetraether lipids or biosynthetic intermediates? Chem. Commun., 48, 841–843, 2012.

765   Koga, Y., Nishihara, M., Morii, H., and Akagawa-Matsushita, M.: Ether polar lipids of methanogenic bacteria: Structures, comparative aspects, and biosynthesis, Microbiol. Rev., 57, 164–182. https://doi.org/10.1128/mr.57.1.164-182., 1993.

Koga, Y., Morii, H.: Recent advances in structural research on ether lipids from Archaea including comparative and physiological aspects, Biochim. Biophys. Acta, 69, 2019–2034. 2005.

770   Kumar, D. M., Woltering, M., Hopmans, E. C., Sinninghe Damsté, J. S., Schouten, S., and Werne, J. P.: The vertical distribution of Thaumarchaeota in the water column of Lake Malawi inferred from core and intact polar tetraether lipids, Org. Geochem., 132, 37–49. 2019.

Lameck, A. S., Skutai, J., and Boros, E.: Review of chemical properties of inland soda and saline waters in East Africa (rift valley region), J. Hydrol. Reg. Stud., 46, 101323, 2023.

775   Langworthy, T. A.: Long-chain diglycerol tetraethers from *Thermoplasma acidophilum*, Biochim. Biophys. Acta (BBA) - Lipid Lipid Met., 487, 37–50. 1977.

Lee, D. H., Kim, J. H., Lee, Y. M., Stadnitskaia, A., Jin, Y. K., Niemann, H., Kim, Y.-G., and Shin, K. H.: Biogeochemical evidence of anaerobic methane oxidation on active submarine mud volcanoes on the continental slope of the Canadian Beaufort Sea, Biogeosciences, 15, 7419–7433, 2018.

780   Lee, H., Fischer, T.P., Muirhead, J.D., Ebinger, C.J., Kattenhorn, S.A., Sharp, Z.D., Kianji, G., Takahata, N., Sano, Y., 2017. Incipient rifting accompanied by the release of subcontinental

lithospheric mantle volatiles in the Magadi and Natron basin, East Africa. J. Volcanol. Geotherm. Res. 346, 118–133.

Leland, H. V., and Berkas, W. R.: Temporal variation in plankton assemblages and physicochemistry of Devils Lake, North Dakota, Hydrobiologia, 377, 57–71, 1998.

Lewis, M.L.: Tropical limnology, Annu. Rev. Ecol. Syst., 18, 159–184, 1987.

Li, M., Peng, C., Zhu, Q., Zhou, X., Yang, G., Song, X., and Zhang, K.: The significant contribution of lake depth in regulating global lake diffusive methane emissions, Water Res., 172, 115465, 2020.

Liu, Y., and Whitman, W. B.: Metabolic, phylogenetic, and ecological diversity of the methanogenic archaea, Ann. NY Acad. Sci., 1125, 171–189, 2008.

Liu, X.-L., Lipp, J.S., Schröder, J.M., Summons, R.E., and Hinrichs, K.-U.: Isoprenoid glycerol dialkanol diethers: a series of novel archaeal lipids in marine sediments, Org. Geochem. 43, 50–55. 2012.

Liu, C., and Wang, P.: The role of algal blooms in the formation of lacustrine petroleum source rocks—evidence from Jiyang depression, Bohai Gulf Rift Basin, eastern China, Palaeogeogr. Palaeoclimatol., Palaeoecol., 388, 15–22, 2013.

Marchant, R., Richer, S., Boles, O., Capitani, C., Courtney-Mustaphi, C. J., Lane, P., Prendergast, M. E., Stump, D., De Cort, G., Kaplan, J. O., Phelps, L., Kay, A., Olago, D., Petek, N., Platts, P. J., Punwong, P., Widgren, M., Wynne-Jones, S., Ferro-Vázquez, C., Benard, J., Boivin, N., Crowther, A., Cuní-Sanchez, A., Deere, N.J., Ekblom, A., Farmer, J., Finch, J., Fuller, D., Gaillard-Lemdahl, M.-J., Gillson, L., Githumbi, E., Kabora, T., Kariuki, R., Kinyanjui, R., Kyazike, E., Lang, C., Lejju, J., Morrison, K.D., Muiruri V., Mumbi, C., Muthoni, R., Muzuka, A., Ndiema, E., Nzabandora, C.K., Iaya Onjala, I., Pas Schrijver, A., Rucina, S., Shoemaker, A., Thornton-Barnett, S., van der Plas, G., Watson, E.E., Williamson, D., Wright, D.: Drivers and trajectories of land cover change in East Africa: Human and environmental interactions from 6000 years ago to present, Earth-Sci. Rev., 178, 322–378, https://doi.org/10.1016/j.earscirev.2017.12.010. 2018.

Marzi, R., Torkelson, B. E., and Olson, R. K.: A revised carbon preference index, Org. Geochem., 20, 1303–1306, 1993.

Melack, J. M., and MacIntyre, S.: Morphometry and physical processes of East African soda lakes,

810   in Soda Lakes of East Africa, edited by: Schagerl, M., Springer, Cham, 61–76, 2016.

Meybeck, M.: Global distribution of lakes, in Physics and Chemistry of Lakes, edited by Lerman, S., Imboden, D.M., and Gat J.L., Springer, Berlin, Heidelberg, 1–35, 1995.

Miller, L. G., Jellison, R., Oremland, R. S., Culbertson, C.W.: Meromixis in hypersaline Mono Lake, California. 3. Biogeochemical response to stratification and overturn,

815   Limnol. Oceanogr., 38, 1040–1051, doi: 10.4319/lo.1993.38.5.1040. 1993.

Morii, H., Eguchi, T., Nishihara, M., Kakinuma, K., Konig, H., Koga, Y.: A novel ether core lipid with H-shaped C-80-isoprenoid hydrocarbon chain from the hyperthermophilic methanogen *Methanothermus fervidus*, Biochim. Biophys. Acta, 1390, 339–345.1998.

Morrissey, A., Scholz, C. A., and Russell, J. M.: Late Quaternary TEX 86 paleotemperatures from the

820   world's largest desert lake, Lake Turkana, Kenya, J. Paleolimnol., 59, 103–117, 2018.

Muirhead, J.D., Kattenhorn, S.A., Lee, H., Mana, S., Turrin, B.D., Fischer, T.P., Kianji, G., Dinde, E., Stamps, D.S.: Evolution of upper crustal faulting assisted by magmatic volatile release during early-stage continental rift development in the East African Rift. Geosphere 12, 1670–1700. 2016.

Muiruri, V.M., Owen, R.B., Lowenstein, T.K., Renaut, R.W., Marchant, R., Rucina, S.M., Cohen, A.C.,

825   Deino, A.L., Sier, M.J., Luo, S., Leet, K., Campisano, C., Rabideaux, N.M., Deocampo, D., Shen, C.-C., Mbuthia, A., Davis, B.C., Aldossari, W., Wang, C.: A million year vegetation history and palaeoenvironmental record from the Lake Magadi Basin, Kenya Rift Valley, Palaeogeogr., Palaeoclimatol., Palaeoecol., 567, 110247, 2021.

Nijaguna, B. T.: Biogas Technology, New Age International, New Delhi, 2006.

830   Norði, K. À., Thamdrup, B., and Schubert, C. J.: Anaerobic oxidation of methane in an iron-rich Danish freshwater lake sediment, Limnol. Oceanogr., 58, 546–554, 2013.

Oliva, M. G., Lugo, A., Alcocer, J., Peralta, L., and del Rosario Sánchez, M.: Phytoplankton dynamics in a deep, tropical, hyposaline lake, in Saline Lakes (Publications from the 7th International Conference on Salt Lakes, Death Valley National Park, California, USA, September 1999), edited by:

835   Melack, J.M., Jellison, R., and Herbst, D.N., Kluwer, Dordecht, 299–306, 2001.

Oremland, R. S., Marsh, L. M., and Polcin, S. (1982). Methane production and simultaneous sulphate reduction in anoxic, salt marsh sediments, Nature, 296, 143–145, 1982.

Oren, A., and Garrity, G. M.: Valid publication of the names of forty-two phyla of prokaryotes, Int. J. Syst. Evol. Microbiol., 71, 005056, 2021.

840   Ortiz, K., Arrowsmith, R., Cohen, A.S., Feibel, C.S., Deino, A., Hill, A., Beck, C.C., Campisano, C.J., Valachovic, J., Kingston, J., 2015, Paleoclimate And Paleoenvironmental Forcing On Early Humans: Loi Analysis Of Three HSPDP Drill Core Sites In Kenya And Ethiopia. Geological Society of America Ann. Mtg., Baltimore, MD

Owen, R. B., Rabideaux, N., Bright, J., Rosca, C., Renaut, R. W., Potts, R., Behrensmeyer, A. K.,
845   Deino, A. L., Cohen, A. S., Muiruri, V., Dommain, R.: Controls on Quaternary geochemical and mineralogical variability in the Koora Basin and South Kenya Rift, Palaeogeogr. Palaeoclim. Palaeoecol, 637, 111986, 2024.

Owen, R. B., Renaut, R. W., Lowenstein, T. K., Stockhecke, M., Rabideaux, N. M., Leet, K., Cohen, A. S., Scott, J. J., Muiruri, V. M.: Pleistocene stratigraphy and sedimentation in the Magadi-Ewaso Nyiro
850   basins, South Kenya Rift, Palaeogeogr. Palaeoclim. Palaeoecol., 112790, 2024.

Owen, R. B., Renaut, R. W., Muiruri, V. M., Rabideaux, N. M., Lowenstein, T. K., McNulty, E. P., Leet, K., Deocampo, D., Luo, S., Deino, A. L., Cohen, A., Sier, M, J., Campisano, C., Shen, C.-C., Billingsley, A., Mbuthia, A., and Stockhecke, M.: Quaternary history of the Lake Magadi Basin, southern Kenya Rift: Tectonic and climatic controls, Palaeogeogr. Palaeoclimatol. Palaeoecol., 518, 97–
855   118, 2019.

Pancost, R. D., Hopmans, E. C., and Sinninghe Damsté, J. S.: Archaeal lipids in Mediterranean cold seeps: molecular proxies for anaerobic methane oxidation, Geochim. Cosmochim. Acta, 65, 1611–1627, 2001.

Parnell, J.: Metal enrichments in solid bitumens: a review. Min. Deposita, 23, 191–199. 1988
860   Paull, C. K., Lorenson, T. D., Borowski, W. S., Ussler Iii, W., Olsen, K., and Rodriguez, N. M.: Isotopic composition of CH_4, CO_2 species, and sedimentary organic matter within samples from the Blake Ridge: Gas source implications, Proc. ODP, Sci. Res., 164, 67–78, 2000.

Pearson, A., Huang, Z., Ingalls, A. E., Romanek, C. S., Wiegel, J., Freeman, K. H., Smittenberg, R. H., and Zhang, C. L.: Nonmarine crenarchaeol in Nevada hot springs, Appl. Environ. Microbiol., 70, 5229–
865   5237. 2004.

Pearson, A., Pi, Y., Zhao, W., Li, W., Li, Y., Inskeep, W., Perevalova, A., Romanek, C., Li, S., Zhang, C.L.: Factors controlling the distribution of archaeal tetraethers in terrestrial hot springs, Appl. Environ. Microbiol., 74, 3523–3532, 2008.

Pecoraino, G., D'Alessandro, W., and Inguaggiato, S.: The other side of the coin: geochemistry of
870 alkaline lakes in volcanic areas, in Volcanic Lakes, edited by: Rouwet, D., Christenson, B., Tassi, F., and Vandemeulebrouck, J., Springer, Berlin, Heidelberg, 219–237, 2015.

Pitcher, A., Rychlik, N., Hopmans, E. C., Spieck, E., Rijpstra, W. I. C., Ossebaar, J., Schouten S., Wagner, M., and Sinninghe Damsté, J. S.: Crenarchaeol dominates the membrane lipids of *Candidatus Nitrososphaera gargensis*, a thermophilic Group I. 1b Archaeon, ISME J., 4, 542–552, 2010.

875 Rattanasriampaipong, R., Zhang, Y. G., Pearson, A., Hedlund, B. P., and Zhang, S.: Archaeal lipids trace ecology and evolution of marine ammonia-oxidizing archaea, Proc. Natl. Acad. Sci., 119(31), e2123193119, 2022.

Reinhardt, M., Goetz, W., Duda, J. P., Heim, C., Reitner, J., and Thiel, V.: Organic signatures in Pleistocene cherts from Lake Magadi (Kenya) – implications for early Earth hydrothermal deposits.
880 Biogeosciences, 16, 2443–2465, 2019.

Renaut, R. W., and Owen, R. B.: The Kenya Rift Lakes: Modern and Ancient: Limnology and Limnogeology of Tropical Lakes in a Continental Rift, Springer, Berlin, Heidelberg, 2023.

Rinke, C., Chuvochina, M., Mussig, A. J., Chaumeil, P. A., Davín, A. A., Waite, D. W., Whitman, W.B., Parks, D.H., and Hugenholtz, P.: A standardized archaeal taxonomy for the Genome Taxonomy
885 Database, Nature Microbiol., 6, 946–959, 2021.

Ritchie, J. C., Eyles, C. H., and Haynes, C. V.: Sediment and pollen evidence for an early to mid-Holocene humid period in the eastern Sahara, Nature, 314, 352–355, 1985.

Robertson, C. E., Spear, J. R., Harris, J. K., and Pace, N. R.: Diversity and stratification of archaea in a hypersaline microbial mat, Appl. Environ. Microbiol., 75, 1801–1810, 2009.

890 Rosentreter, J. A., Borges, A. V., Deemer, B. R. , Holgerson, M. A., Liu, S., Song, C., Melack, J., Raymond, P. A., Duarte, C. M., Allen, G. A., Olefeldt, D., Poulter, B., Battin, T. I., and Eyre, B. D.: Half of global methane emissions come from highly variable aquatic ecosystem sources, Nature Geosci.,14, 225–230, https://doi.org/10.1038/s41561-021-00715-2, 2021.

Rütters, H., Sass, H., Cypionka, H., and Rullkötter, J.: Phospholipid analysis as a tool to study complex microbial communities in marine sediments, J. Microbiol. Meth. 48, 149–160, 2002.

Schagerl, M. (Ed.): Soda Lakes of East Africa, Springer, Cham, 2016.

Schagerl, M., and Renaut, R. W.: Dipping into the soda lakes of East Africa, in Soda Lakes of East Africa, edited by: Schagerl, M., Springer, Cham, 3–34, 2016.

Schouten, S., Hopmans, E. C., Schefuß, E., and Sinninghe Damsté, J. S.: Distributional variations in marine crenarchaeotal membrane lipids: a new tool for reconstructing ancient sea water temperatures? Earth Planet. Sci. Lett, 204, 265–274, 2002.

Schouten, S., Wakeham, S. G., Hopmans, E. C., and Sinninghe Damsté, J. S.: Biogeochemical evidence that thermophilic archaea mediate the anaerobic oxidation of methane, Appl. Environ. Microbiol., 69, 1680–1686, 2003.

Schouten, S., Hopmans, E. C., and Sinninghe Damsté, J. S.: The organic geochemistry of glycerol dialkyl glycerol tetraether lipids: A review, Org. Geochem., 54, 19–61, 2013.

Schubotz, F., Meyer-Dombard, D. R., Bradley, A. S., Fredricks, H. F., Hinrichs, K. U., Shock, E. L., and Summons, R. E.: Spatial and temporal variability of biomarkers and microbial diversity reveal metabolic and community flexibility in streamer biofilm communities in the Lower Geyser Basin, Yellowstone National Park, Geobiology, 11, 549-569, 2013.

Shah, S. R., Mollenhauer, G., Ohkouchi, N., Eglinton, T. I., and Pearson, A.: Origins of archaeal tetraether lipids in sediments: Insights from radiocarbon analysis, Geochim. Cosmochim. Acta, 72, 4577–4594, 2008.

Shanahan, T. M., McKay, N. P., Hughen, K. A., Overpeck, J. T., Otto-Bliesner, B., Heil, C. W., King, J., Scholz, C.A., and Peck, J.: The time-transgressive termination of the African Humid Period, Nature Geosci., 8, 140–144, 2015.

Sinninghe Damsté, J. S., Schouten, S., Hopmans, E. C., Van Duin, A. C., and Geenevasen, J. A.: Crenarchaeol, J. Lipid Res., 43, 1641–1651, 2002.

Sinninghe Damsté, J. S., Rijpstra, W. I. C., Hopmans, E. C., Jung, M. Y., Kim, J. G., Rhee, S. K., Steiglmeier, M., and Schleper, C. (2012). Intact polar and core glycerol dibiphytanyl glycerol tetraether lipids of group I. 1a and I. 1b Thaumarchaeota in soil, Appl. Environ. Microbiol., 78, 6866–6874, 2012.

Sikes, N. E.: Early hominid habitat preferences in East Africa: paleosol carbon isotopic evidence, J. Hum. Evol., 27, 25–45, 1994.

Sivan, O., Adler, M., Pearson, A., Gelman, F., Bar-Or, I., John, S. G., and Eckert, W.: Geochemical evidence for iron-mediated anaerobic oxidation of methane, Limnol. Oceanogr., 56, 1536–1544, 2011

Smith, J. M., Green, S. J., Kelley, C. A., Prufert-Bebout, L., and Bebout, B. M.: Shifts in methanogen community structure and function associated with long-term manipulation of sulfate and salinity in a hypersaline microbial mat, Environ. Microbiol., 10, 386–394, 2008.

Sorokin, D. Y., Foti, M., Pinkart, H. C., and Muyzer, G.: Sulfur-oxidizing bacteria in Soap Lake (Washington State), a meromictic, haloalkaline lake with an unprecedented high sulfide content, Appl. Environ. Microbiol., 73, 451–455, 2007.

Sorokin, D. Y., Abbas, B., Geleijnse, M., Pimenov, N. V., Sukhacheva, M. V., and van Loosdrecht, M. C.: Methanogenesis at extremely haloalkaline conditions in the soda lakes of Kulunda Steppe (Altai, Russia), FEMS Microbiol. Ecol., 91, fiv016, 2015.

Sturt, H. F., Summons, R. E. Smith, K., Elvert, M. and Hinrichs, K. U.: Intact polar membrane lipids in prokaryotes and sediments deciphered by high-performance liquid chromatography/electrospray ionization multistage mass spectrometry - new biomarkers for biogeochemistry and microbial ecology, Rapid Comm. Mass Spec. 18, 617–28, 2004.

Straka, L. L., Meinhardt, K. A., Bollmann, A., Stahl, D. A., and Winkler, M. K.: Affinity informs environmental cooperation between ammonia-oxidizing archaea (AOA) and anaerobic ammonia-oxidizing (Anammox) bacteria, ISME J., 13, 1997–2004, 2019.

Summons, R. E., Franzmann, P. D., and Nichols, P. D.: Carbon isotopic fractionation associated with methylotrophic methanogenesis, Org. Geochem., 28, 465–475, 1998.

Sun, Y., Liu, C., Lin, M., Li, Y., and Qin, P.: Geochemical evidences of natural gas migration and releasing in the Ordos Basin, China, Energy Explor. Exploit., 27, 1–13, 2009.

Talling J. F., and Lemoalle, J.: Ecological Dynamics of Tropical Inland Waters, Cambridge University Press, Cambridge, 1998.

Taylor, K. W., Huber, M., Hollis, C. J., Hernandez-Sanchez, M. T., and Pancost, R. D.: Re-

evaluating modern and Palaeogene GDGT distributions: Implications for SST reconstructions, Global

950 Planet. Change, 108, 158–174. 2013.

Turich, C., Freeman, K. H., Bruns, M. A., Conte, M., Jones, A. D., Wakeham, S. G.: Lipids of marine

Archaea: patterns and provenance in the water-column and sediments, Geochem. Cosmochim. Acta, 71,

3272–3291, https://doi.org/10.1016/j.gca.2007.04.013, 2007.

Verpoorter, C., Kutser, T., Seekell, D. A., and Tranvik, L. J.: A global inventory of lakes based on high-

955 resolution satellite imagery, Geophys. Res. Lett., 41, 6396–6402, 2014.

Volkova, N. I.: Geochemistry of rare elements in waters and sediments of alkaline lakes in the

Sasykkul depression, East Pamirs, Chem. Geol., 147, 265–277, 1998.

Wakeham, S. G., Lewis, C. M., Hopmans, E. C., Schouten, S., and Sinninghe Damsté, J. S.: Archaea

mediate anaerobic oxidation of methane in deep euxinic waters of the Black Sea, Geochim.

960 Cosmochim. Acta, 67, 1359–1374. 2003.

Weijers, J. W., Lim, K. L., Aquilina, A., Sinninghe Damsté, J. S., and Pancost, R. D.:

Biogeochemical controls on glycerol dialkyl glycerol tetraether lipid distributions in sediments

characterized by diffusive methane flux, Geochem., Geophys., Geosyst., 12,

https://doi.org/10.1029/2011GC003724, 2011.

965 Werne, J. P., Zitter, T., Haese, R. R., Aloisi, G., Bouloubassi, I., Heijs, S., Fiala-Medioni, A., Pancost,

R.D., Sinninghe Damsté, J. S., de Lange, G., Forney, L.J., Gottschal, J.C., Foucher, J.-P., Mascle, J.,

Woodside, J., and the MEDINAUT and MEDINETH Shipboard Scientific Parties: Life at cold seeps: A

synthesis of ecological and biogeochemical data from Kazan mud volcano, eastern Mediterranean Sea,

Chem. Geol., 205, 367–390, 2004.

970 Williamson, D., Taieb, M., Damnati, B., Icole, M., and Thouveny, N.: Equatorial extension of the

Younger Dryas event: rock magnetic evidence from Lake Magadi (Kenya), Global Planet. Change, 7,

235–242, 1993.

Woulds, C., Bell, J. B., Glover, A. G., Bouillon, S., Brown L.S.: Benthic carbon fixation and cycling

in diffuse hydrothermal and background sediments in the Bransfield Strait, Antarctica, Biogeosciences

975 17, 1–12, https://doi.org/10.5194/bg-17-1-2020. 2020.

Wright, H. E.: A square-rod piston sampler for lake sediments, J. Sediment. Petrol., 37, 975–976, 1967.

Wright H. E.: Cores of soft lake sediments, Boreas, 9, 107–114. https://doi.org/10.1111/j.1502-3885.1980.tb01032.x., 1980.

Wynn, J. G., Lowenstein, T. K., Renaut, R. W., Owen, R. B. and McNulty, E. P.: Superheavy pyrite
980   formation in hypersaline lakes of East Africa: a paleosalinity proxy for Lake Magadi HSPDP cores, Geol. Soc. Am. Abstr. Progr., 50, Paper 184–3, https://doi.org/10.1130/abs/2018AM-323852, 2018.

Xia, L., Cao, J., Hu, W., Stüeken, E. E., Wang, X., Yao, S., Zhi, D., Tang, Y., Xiang, B., and He, W.: Effects on global warming by microbial methanogenesis in alkaline lakes during the Late Paleozoic Ice Age (LPIA), Geology, 51, 935–940, 2023.

985   Zhang, Y. G., Zhang, C. L., Liu, X. L., Li, L., Hinrichs, K. U., and Noakes, J. E.: Methane Index: A tetraether archaeal lipid biomarker indicator for detecting the instability of marine gas hydrates, Earth Planet. Sci. Lett., 307, 525–534, 2011.

Zhuang, G. C., Elling, F. J., Nigro, L. M., Samarkin, V., Joye, S. B., Teske, A., and Hinrichs, K. U.: Multiple evidence for methylotrophic methanogenesis as the dominant methanogenic pathway in
990   hypersaline sediments from the Orca Basin, Gulf of Mexico. Geochim. Cosmochim. Acta, 187, 1–20. 2016.
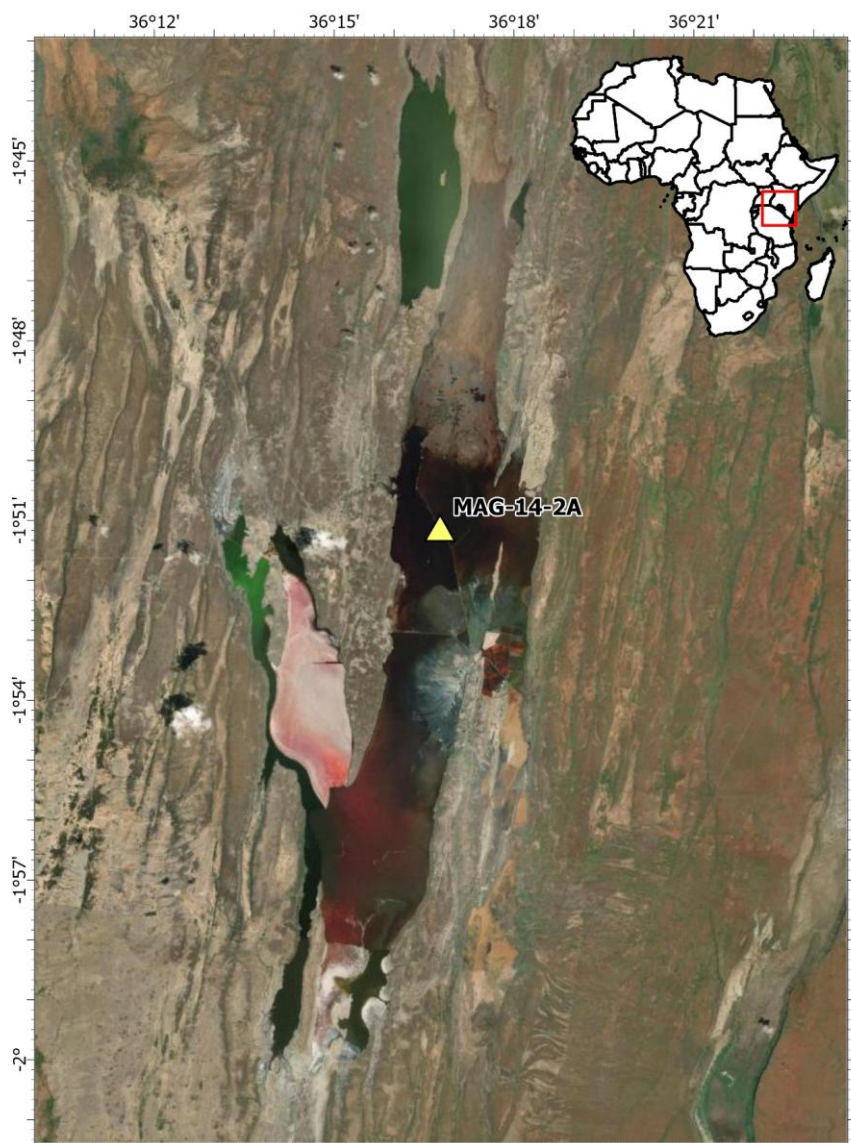
Figure 1. Map of the drilling location of MAG-14-2A (yellow triangle) in Lake Magadi for the Hominin Sites and Paleolakes Drilling Project (HSPDP).
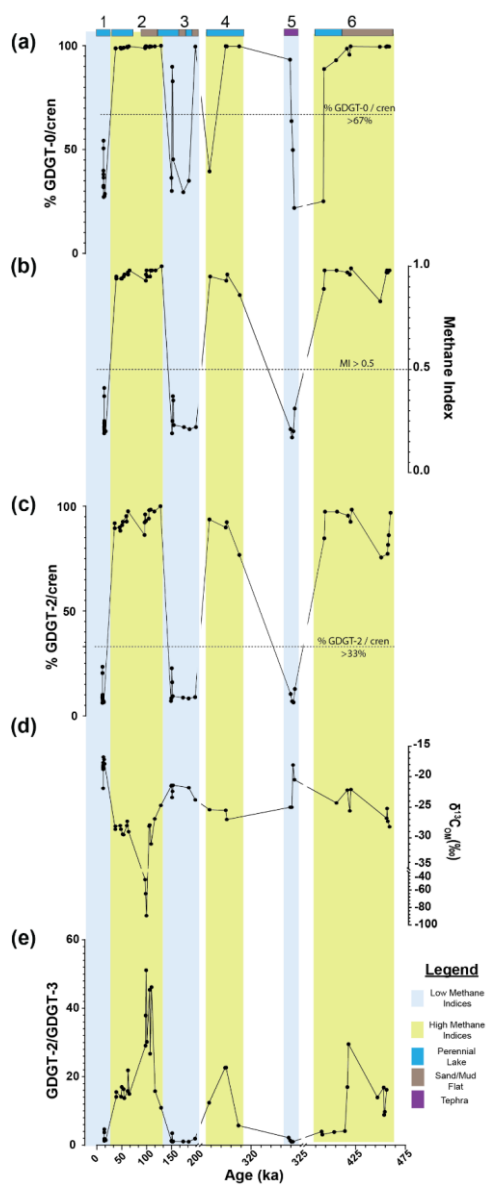
Figure 2. Downcore variations in Lake Magadi of the **a)** % 0/ /Cren, **b)** MI, **c)** % 2/ /Cren, **d)** bulk $\delta^{13}C_{OM}$, and **e)** the GDGT-2/ /GDGT-3 ([2]/ /[3]) values from ca. 14.9 to 456 ka. Sections 1, 3, and 5 are low MI intervals outlined in blue, the high MI intervals in Sections 2, 4, and 6 are in yellow. ~~Checkered patterns indicate periods of tuffaceous silt deposit, which align with the low MI intervals.~~ Bands at the top of the graph indicate the inferred (via Renaut and Owen, 2023) lake levels and major inputs with dark blue indicating a perennial lake, brown indicating a sand or mud flat, and purple indicating tephra. Dotted lines on each section denote the cut-off points for methane related indices MI (>-0.5), %-GDGT-2/ /cren (>-33-%), and %-GDGT-0 / cren (>-67-%). See Section 2.3.2 for more details. Note the breaks in the X-axis scale.
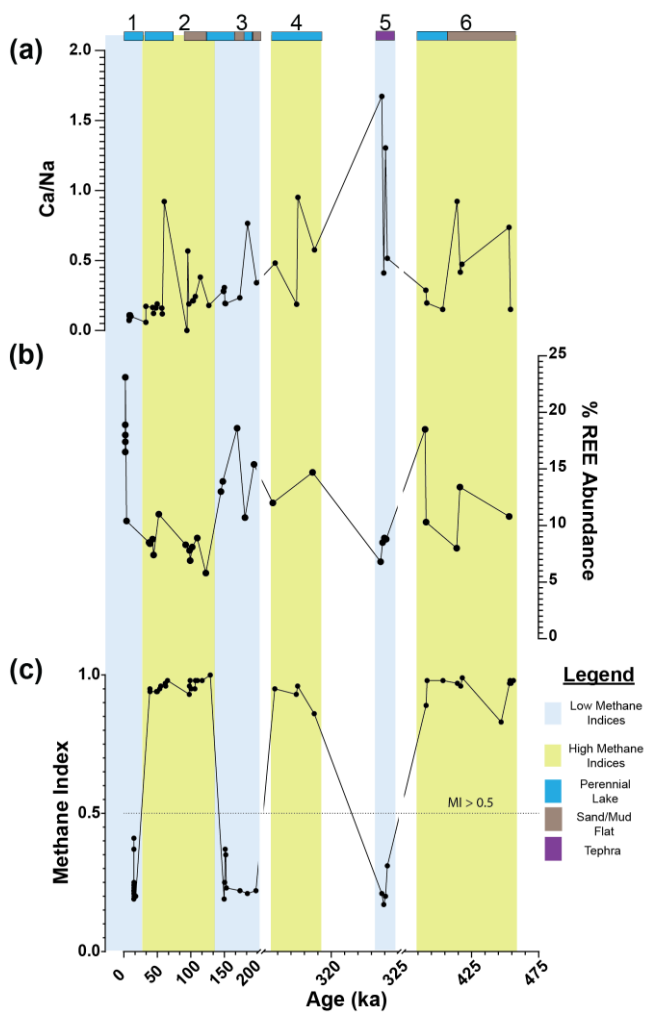
Figure 3. Downcore plot for Lake Magadi of **a)** Ca/Na, **b)** %-REE abundance, and **c)** MI. Values range from ca. 14.9 to 456 ka and Sections 1, 3, and 5 are outlined in blue reflecting a low MI interval, while high MI intervals are outlined in yellow. ~~The checkered pattern is indicative of periods of higher inferred hydrothermal flow.~~ Bands at the top of the graph indicate the inferred (via Renaut and Owen, 2023) lake

levels and major inputs with dark blue indicating a perennial lake, brown indicating a sand or mud flat, and purple indicating tephra. The dotted line on the MI plot **(c)** denotes the cutoff point >-0.5 for values significantly affected by methane cycling archaea. Note the breaks in the X-axis scale and in the Y-axis scale for the $\delta^{13}C_{OM}$. REE values are from Owen et al. (2019).
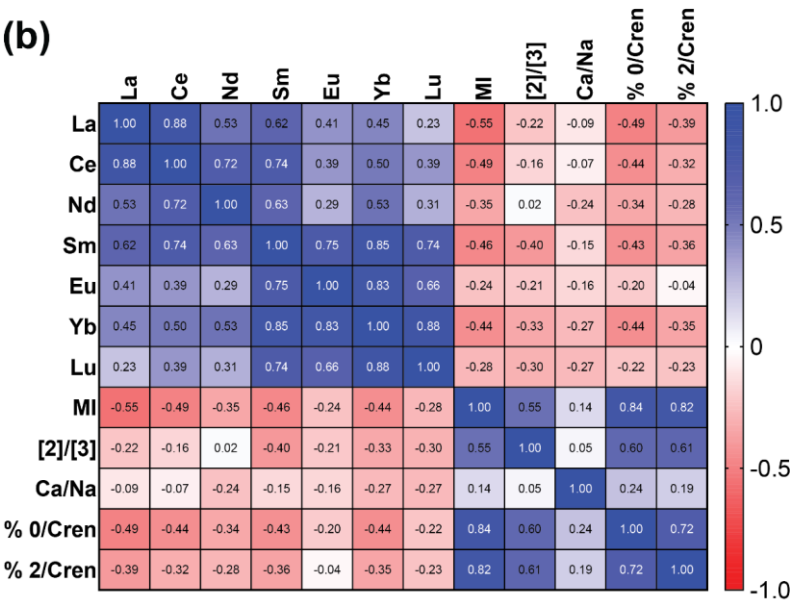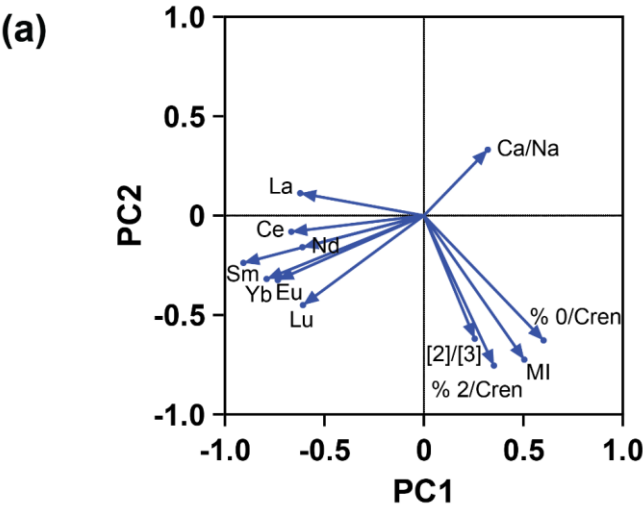
Figure 4. Both **a)** PCA and **b)** Spearman Correlation Matrix showing the relationship between methane related indices (MI and [2] / [3]) and REEs (La, Ce, Nd, Sm, Eu, Tb, Yb, and Lu) in the sampled intervals of the core. A negative relationship is seen between the methane indices and REEs as shown by opposing eigenvectors on the PCA **(a)** and negative r values on the correlation matrix **(b)**. REE values are from Owen et al. (2019).
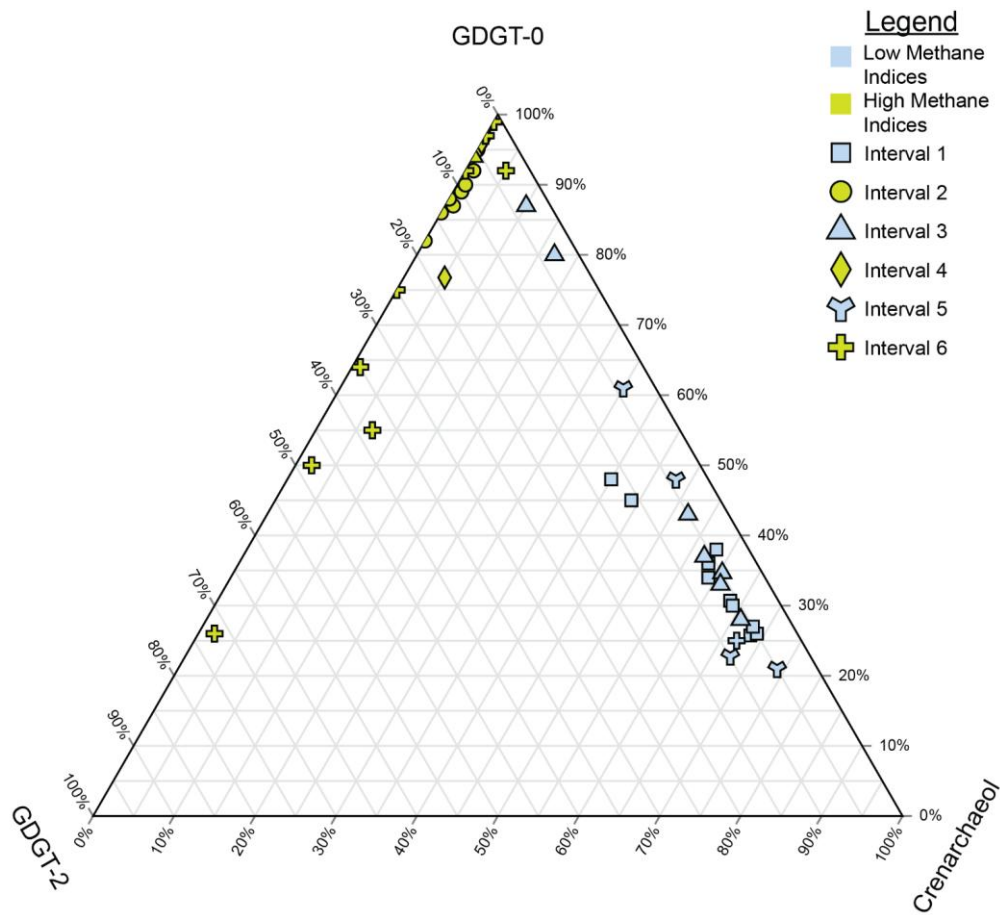
1025   **Figure 5.** Ternary plot of crenarchaeol, GDGT-0, and GDGT-2, which are used to calculate the methane indices. Samples are split by both their interval (denoted by their shape) and whether they are from a high MI (yellow) or low MI (blue) interval. Higher proportions of GDGT-0 indicate methanogenic inputs, higher GDGT-2 indicate methanotrophy, and higher crenarchaeol indicates more mesophilic conditions influenced by hot springs.

1030